

Supporting Information

## **Porphyrinic Probe for Fluorescence “Turn-On” Monitoring of Cu<sup>+</sup> in Aqueous Buffer and Mitochondria**

Xiao-Qin Yi<sup>1,2</sup>, Yuan-Fan He<sup>1</sup>, Yu-Sheng Cao<sup>1</sup>, Wang-Xing Shen<sup>1</sup>, Yuan-Yuan Lv<sup>1,\*</sup>

<sup>1</sup>School of Medicine, Zhejiang University City College, Hangzhou, Zhejiang 310015, People's Republic of China

<sup>2</sup>College of Pharmacy, Zhejiang University, Hangzhou, Zhejiang 310027, People's Republic of China

---

\* Corresponding author. Fax: + 86 571 8801 8442; e-mail: [lvyy@zucc.edu.cn](mailto:lvyy@zucc.edu.cn) (Y.-Y. Lv)

## Table of Contents

### Apparatus and Characterizations

#### Synthetic Procedures

**Figure S1.**  $^1\text{H}$  NMR spectrum of compound  $\beta$ -ATPPS in  $\text{DMSO-}d_6$ .

**Figure S2.**  $^{13}\text{C}$  NMR spectrum of compound  $\beta$ -ATPPS in  $\text{DMSO-}d_6$ .

**Figure S3.** Mass spectrum of compound  $\beta$ -ATPPS.

**Figure S4.**  $^1\text{H}$  NMR spectrum of compound  $\text{Zn}\beta$ -ATPPS in  $\text{DMSO-}d_6$ .

**Figure S5.**  $^{13}\text{C}$  NMR spectrum of compound  $\text{Zn}\beta$ -ATPPS in  $\text{DMSO-}d_6$ .

**Figure S6.** Mass spectrum of compound  $\text{Zn}\beta$ -ATPPS.

**Figure S7.**  $^1\text{H}$  NMR spectrum of compound (1a) in  $\text{CDCl}_3$ .

**Figure S8.**  $^{13}\text{C}$  NMR spectrum of compound (1a) in  $\text{CDCl}_3$ .

**Figure S9.** Mass spectrum of compound (1a).

**Figure S10.**  $^1\text{H}$  NMR spectrum of compound (2) in  $\text{DMSO-}d_6$ .

**Figure S11.**  $^{13}\text{C}$  NMR spectrum of compound (2) in  $\text{DMSO-}d_6$ .

**Figure S12.** Mass spectrum of compound (2).

**Figure S13.**  $^1\text{H}$  NMR spectrum of compound ZPSN in  $\text{DMSO-}d_6$ .

**Figure S14.**  $^{13}\text{C}$  NMR spectrum of compound ZPSN in  $\text{DMSO-}d_6$ .

**Figure S15.** Mass spectrum of compound ZPSN.

**Figure S16.**  $^1\text{H}$  NMR spectrum of compound PSN in  $\text{DMSO-}d_6$ .

**Figure S17.**  $^{13}\text{C}$  NMR spectrum of compound PSN in  $\text{DMSO-}d_6$ .

**Figure S18.** Mass spectrum of compound PSN.

**Figure S19.**  $^1\text{H}$  NMR spectrum of compound ZPN in  $\text{DMSO-}d_6$ .

**Figure S20.**  $^{13}\text{C}$  NMR spectrum of compound ZPN in  $\text{DMSO-}d_6$ .

**Figure S21.** Mass spectrum of compound ZPN.

**Figure S22.** Partial  $^1\text{H}$  NMR spectra of compounds ZPSN and PSN in  $\text{DMSO-}d_6$ .

#### Solubility of ZPSN in PBS

**Figure S23.** Absorbance (at 430 nm) vs. different concentrations of ZPSN in 20 mM PBS at pH 7.0.

**Figure S24.** Job's plot for ZPSN with  $\text{Cu}^+$  in 20 mM PBS at pH 7.0.  $\Delta A_{415\text{nm}}$  is the absorbance changes at 415 nm during titration with a total concentration of ZPSN and  $\text{Cu}^+$  kept at 2  $\mu\text{M}$  ( $X_M = [\text{Cu}^+]/([\text{ZPSN}] + [\text{Cu}^+])$ ).

## Determination of the Dissociation Constant ( $K_d$ )

**Figure S25.** Benesi-Hildebrand plot (linear plot) for  $\text{Cu}^+$ -bound ZPSN.

**Figure S26.** Fluorescence response upon titration of  $\text{Cu}^+$  into ZPSN solution ( $2\ \mu\text{M}$ ) in PBS ( $20\ \text{mM}$ , pH 7.0) in the presence of GSH ( $1\ \text{mM}$ ). Inset: plot of  $\Delta F_{623}$  versus ( $\text{Cu}^+$ : ZPSN) for the titration of ZPSN ( $2\ \mu\text{M}$ ) in the presence of  $1\ \text{mM}$  GSH.

**Figure S27.** Fluorescence emission intensity at  $623\ \text{nm}$  of free ZPSN ( $2\ \mu\text{M}$ ) and in the presence of  $\text{Cu}^+$  ( $1\ \text{equiv.}$ ) at different pHs.

## Calculation of the Detection Limit

**Figure S28.** Linear calibration curve between the changes in fluorescence intensity at  $623\ \text{nm}$  ( $\Delta F$ ) and the concentration of  $\text{Cu}^+$ .

**Figure S29.**  $^1\text{H}$ NMR spectra of ZPSN in the absence and presence of  $1\ \text{equiv.}$  of  $\text{Cu}^+$  in  $\text{DMSO-}d_6$ .

**Figure S30.** Mass spectrum of ZPSN/ $\text{Cu}^+$  complex.

**Figure S31.** Fluorescence spectra of ZPN ( $2\ \mu\text{M}$ ) and ZPSN ( $2\ \mu\text{M}$ ) in the presence of  $\text{Cu}^+$  in PBS ( $20\ \text{mM}$ , pH 7.0),  $\lambda_{\text{ex}} = 415\ \text{nm}$ . Black lines: ZPN ( $2\ \mu\text{M}$ ) with increasing concentrations of  $\text{Cu}^+$  ( $\mu\text{M}$ ) ( $0, 0.5, 0.75, 1, 1.5, 2, 3, 4$ ); red line : ZPSN ( $2\ \mu\text{M}$ ) with  $4\ \mu\text{M}$   $\text{Cu}^+$ .

**Figure S32.** Fluorescent intensity of ZPSN ( $2\ \mu\text{M}$ ) at  $623\ \text{nm}$  in the absence and upon addition of  $1\ \text{equiv.}$  of  $\text{Cu}^+$  as a function of time in PBS ( $20\ \text{mM}$ , pH 7.0).

## Cytotoxicity Test

**Figure S33.** Cell viability of HeLa cells with different concentrations of ZPSN ( $0, 1, 2, 5, 10, 50, 100\ \mu\text{M}$ ) for  $24\ \text{h}$ .

**Figure S34.** Confocal fluorescence imaging of  $\text{Cu}^+$  in A549 cells. (a) Cells incubated with ZPSN ( $2\ \mu\text{M}$ ) for  $20\ \text{min}$ ; (b) Cells pretreated with  $0.1\ \text{mM}$   $\text{CuCl}_2$  in growth media for  $7\ \text{h}$  at  $37\ ^\circ\text{C}$  and stained with  $2\ \mu\text{M}$  ZPSN for an additional  $20\ \text{min}$ ; (c) Cells pretreated with  $0.1\ \text{mM}$   $\text{CuCl}_2$  for  $7\ \text{h}$ , further incubated with  $2\ \mu\text{M}$  ZPSN for  $20\ \text{min}$ , and subsequently treated with the competing  $\text{Cu}^+$  chelator TAHD ( $0.1\ \text{mM}$ ) for  $15\ \text{min}$  at  $37\ ^\circ\text{C}$ . (a-1), (b-1), (c-1) Bright-field images; (a-2), (b-2), (c-2) Fluorescence images collected at  $600\text{--}650\ \text{nm}$ ; (a-3), (b-3), (c-3) Merged images of the bright field and fluorescence field. (Scale bars,  $20\ \mu\text{m}$ ;  $\lambda_{\text{ex}} = 488\ \text{nm}$ ).

**Figure S35.** Colocalization experiments of ZPSN in mitochondria. Confocal images of A549 cells pretreated with  $\text{CuCl}_2$  ( $0.1\ \text{mM}$ ) for  $7\ \text{h}$  followed by incubation with MitoTracker Green ( $100\ \text{nM}$ ) for  $20\ \text{min}$  and ZPSN ( $2\ \mu\text{M}$ ) for  $20\ \text{min}$ . (a) Images were collected at  $500\text{--}550\ \text{nm}$ . (b) Images were collected at  $600\text{--}650\ \text{nm}$ . (c) Colocalized images. (Scale bars,  $20\ \mu\text{m}$ ;  $\lambda_{\text{ex}} = 488\ \text{nm}$ ).

## References

**Apparatus and Characterizations.** NMR spectra were obtained on a Bruker (Advance DMX500) NMR spectrometer (Bruker-Franzen Analytik GmbH, Germany). High resolution mass spectroscopy (HRMS) were performed on a Bruker Esquire 3000 Plus spectrophotometer (Bruker-Franzen Analytik GmbH, Germany). Absorbance measurements were obtained using a Shimadzu UV 2450 UV–vis spectrophotometer (Shimadzu, Japan). Fluorescence measurements were collected using a Shimadzu RF-5301 PC fluorescence spectrophotometer (Shimadzu, Japan). Both excitation and emission slits measured at 3 nm. Quantum yields were determined using 5,10,15,20-*tetra*(4-sulfonatophenyl)-porphyrin (TPPS<sub>4</sub>) in 50 mM HEPES buffer (pH 7.0), 100 mM KCl as a fluorescence standard ( $\Phi_{Ref} = 0.16$ ). Fluorescence lifetime measurements were performed using a time correlated single photon counting (TCSPC) spectrometer (Horiba Scientific, UK) equipped with a pulsed laser diode as the excitation source (pulse width: 10 ps). The sample was excited with 415 nm and emission was collected at corresponding emission wavelength. A PMT based detector (TBX-04) was used for detection of the emitted photons through a monochromator. The instrument response was ascertained experimentally by collecting the scattered light from a TiO<sub>2</sub> suspension in water. The instrument response function (IRF) thus measured was ~200 ps. The decays were analyzed using DAS-6 (Horiba Scientific, UK) analysis software. The fluorescence decay curves were analyzed by non-linear least-square iterative convolution method using the following Eq. (S1) based on chi-square ( $\chi^2$ ) minimization algorithm semi-logarithmic plot. The reliability of fitting was checked by numerical value of  $\chi^2$  (with an acceptable range of 1.0–1.3).

$$y(t) = \sum_i a_i \exp(-t/\tau_i) \quad (S1)$$

where  $y(t)$  is decay,  $i$  is the number of discrete emissive species,  $a_i$  is the pre-exponential factor, and  $\tau_i$  is the excited state lifetime associated with the  $i$ th component, respectively. Cell imaging was investigated using laser scanning confocal microscopy (LSCM) with a Leica TCS SP5 confocal setup mounted on a Leica DMI 6000 CS inverted microscope (Leica Microsystems, Germany) and was operated under the Leica Application Suite Advanced Fluorescence (LASAF) program. All pH measurements were made with a PHS-25 acidometer (Shanghai Leici Instrument Co., China). All solutions were prepared and diluted using ultrapure water supplied through a Millipore Milli-Q water purification system (Billerica, USA) (with a resistivity of 18 M $\Omega$ ). Dialysis was performed with Spectra/ Por<sup>®</sup> Dialysis Membrane (USA).

## Synthetic Procedures

### 1. Synthesis of 2-amino-5,10,15,20-(4-sulfonatophenyl)-porphyrin ( $\beta$ -ATPPS)

2-Amino-5,10,15,20-tetraphenyl-porphyrin Zinc(II) (Zn $\beta$ -ATPP) was synthesized according to a previously reported procedure.<sup>1</sup> Zn $\beta$ -ATPP (0.75 g, 1.08 mmol) was added in a 250 mL round-bottom flask with 35 mL of concentrated sulfuric acid. The mixture was heated up to 75°C in

an oil bath for 8 hours. After the reaction, the porphyrin solution was carefully poured into a beaker of ice, diluted, and slowly neutralized with 1.0 M NaOH until the solution turned deep red. Then extracted with CH<sub>2</sub>Cl<sub>2</sub> to separate the unreacted Znβ-ATPP. Extensive purification was performed by ultracentrifugation filtration the aqueous phase in a 1 000 MWCO membrane for several times with ultrapure water to remove the salt. The product was further purified by reversephase column chromatography (RP-18), using a H<sub>2</sub>O/MeOH gradient (0 % MeOH to 60 % MeOH) to yield, after lyophilization, a red solid product (yield: 88.3 %). As reflux with strong acid is a commonly used method for demetallization of metalloporphyrins, the obtained product should be metal free form of 2-amino-5,10,15,20-(4-sulfonatophenyl)-porphyrin (β-ATPPS) as sodium salt. <sup>1</sup>H NMR (500 MHz, DMSO-*d*<sub>6</sub>) δ 8.68-8.79 (m, 6H), 8.57 (s, 1H), 8.16 (d, 2H, *J* = 7.0 Hz), 8.11 (d, 2H, *J* = 7.0 Hz), 7.64-7.78 (m, 8H), 7.57 (d, 4H, *J* = 7.2 Hz), 4.72 (s, 2H), -2.83 (s, 2H). <sup>13</sup>C NMR (125 MHz, DMSO-*d*<sub>6</sub>) δ 151.40, 145.38, 144.55, 144.10, 135.32, 135.12, 131.62, 131.32, 131.13, 128.93, 126.20, 124.83, 124.42, 123.04, 122.86, 119.09, 105.40. MS (ESI) *m/z* calcd for [M-4Na]<sup>4-</sup> C<sub>44</sub>H<sub>27</sub>N<sub>5</sub>O<sub>12</sub>S<sub>4</sub><sup>4-</sup>: 236.2640. Found: 236.2648. Anal. Calcd (%) for C<sub>44</sub>H<sub>27</sub>N<sub>5</sub>Na<sub>4</sub>O<sub>12</sub>S<sub>4</sub>: C, 50.92; H, 2.62; N, 6.75. Found: C, 51.01; H, 2.57; N, 6.59.

## 2. Synthesis of 2-amino-5,10,15,20-(4-sulfonatophenyl)-porphyrin Zinc (II) (Znβ-ATPPS)

β-ATPPS (0.6 g, 0.58 mmol) and zinc(II) acetate dihydrate (0.64 g, 2.32 mmol) was added to 95 ml of DMF. The solution was refluxed for 4 hours, cooled to room temperature, and then the solvent was removed under reduced pressure. The precipitate was dissolved in water and dialysis in a 1 000 MWCO membrane for several hours to remove the bulk excess salt. The dialyzed solution was purified by reversephase column chromatography (RP-18) using a H<sub>2</sub>O/MeOH gradient (0 % MeOH to 40 % MeOH). The product was run through an Amberlite IR120, Na<sup>+</sup> form, to further remove the possible free Zn<sup>2+</sup>. Finally, it was lyophilized to give the final product (92.1 %) as sodium salt. <sup>1</sup>H NMR (500 MHz, DMSO-*d*<sub>6</sub>) δ 8.75-8.86 (m, 6H), 8.70 (s, 1H), 8.21 (d, 2H, *J* = 6.8 Hz), 8.16 (d, 2H, *J* = 6.8 Hz), 7.72-7.84 (m, 8H), 7.61 (d, 4H, *J* = 7.1 Hz), 4.78 (s, 2H). <sup>13</sup>C NMR (125 MHz, DMSO-*d*<sub>6</sub>) δ 153.33, 149.91, 147.94, 147.53, 134.95, 134.69, 132.35, 132.12, 131.91, 129.03, 127.29, 124.83, 124.56, 121.21, 119.98, 117.31, 107.12. MS (ESI) *m/z* calcd for [M-4Na]<sup>4-</sup> C<sub>44</sub>H<sub>25</sub>N<sub>5</sub>O<sub>12</sub>S<sub>4</sub>Zn<sup>4-</sup>: 251.7424. Found: 251.7418. Anal. Calcd (%) for C<sub>44</sub>H<sub>25</sub>N<sub>5</sub>Na<sub>4</sub>O<sub>12</sub>S<sub>4</sub>Zn: C, 47.99; H, 2.29; N, 6.36. Found: C, 47.84; H, 2.32; N, 6.42.

## 3. Synthesis of *N*-(pyridin-2-ylmethyl)-2-(ethylthio) ethanamine (1a)

2-(Ethylthio)ethanamine (0.95 g, 9 mmol) was dissolved in 15 mL of dry acetonitrile, and the solution was added dropwise to a stirred mixture of 2-(bromomethyl)pyridine (3.08 g, 18 mmol),

NaHCO<sub>3</sub> (1.51 g, 18 mmol) and KI (1.49 g, 9 mmol) at room temperature under N<sub>2</sub>. After overnight stirring, the solvent was evaporated under reduced pressure. Then the residue was dissolved in CH<sub>2</sub>Cl<sub>2</sub> and washed three times with saturated NaHCO<sub>3</sub> solution and water. The combined organic phase was dried over anhydrous MgSO<sub>4</sub>, and the solvent was removed under reduced pressure. Purification by silica gel column chromatography using CH<sub>2</sub>Cl<sub>2</sub>/CH<sub>3</sub>OH (v/v, 95/5) as the eluent to yield compound (1) as a dark yellow oil (yield 67.2 %). <sup>1</sup>H NMR (500 MHz, CDCl<sub>3</sub>): δ 7.75 (1H, t, *J* = 7.4 Hz), 7.64 (1H, t, *J* = 7.4 Hz), 7.46 (1H, d, *J* = 6.8 Hz), 7.39 (1H, d, *J* = 6.8 Hz), 3.82 (2H, s), 3.48-3.53 (m, 1H), 2.82 (2H, t, *J* = 7.4 Hz), 2.66 (2H, t, *J* = 7.4 Hz), 2.50 (2H, q, *J* = 7.2 Hz), 1.25 (3H, t, *J* = 7.2 Hz). <sup>13</sup>C NMR (125 MHz, CDCl<sub>3</sub>) δ 160.36, 148.59, 148.49, 139.73, 124.52, 121.60, 121.44, 52.87, 52.23, 32.58, 25.00, 15.10. MS (ESI) *m/z* calcd for [M+H]<sup>+</sup> C<sub>10</sub>H<sub>17</sub>N<sub>2</sub>S<sup>+</sup>: 197.1112. Found: 197.1208.

#### 4. Synthesis of 2-bromoacetamide-5,10,15,20-tetra-(4-sulfonatophenyl)-porphyrin Zinc (II) (2)

Bromoacetyl bromide (0.17 mL, 2.1 mmol) was dissolved in dry DMF (10 mL) at 0 °C, and a stirred mixture of Znβ-ATPPS (0.5 g, 0.5 mmol) and triethylamine (0.29 mL) in DMF (10 mL) were added slowly under N<sub>2</sub>, the reaction mixture was kept stirring over night at room temperature. Then the mixture was concentrated under reduced pressure. The precipitate was dissolved in water and performed by ultracentrifugation filtration in a 1 000 MWCO membrane for several times with ultrapure water to remove the salt. The product was further purified by reversephase column chromatography (RP-18) using a H<sub>2</sub>O/MeOH gradient (0 % MeOH to 50 % MeOH), and was lyophilized to obtain (2) as sodium salt in 89.0 % yield. <sup>1</sup>H NMR (500 MHz, DMSO-*d*<sub>6</sub>) δ 9.57 (s, 1H), 8.79-8.85 (m, 6H), 8.66 (s, 1H), 8.17-8.21 (m, 4H), 7.88-8.07 (m, 8H), 7.83 (d, 4H, *J* = 7.4 Hz), 4.41 (s, 2H). <sup>13</sup>C NMR (125 MHz, DMSO-*d*<sub>6</sub>) δ 166.57, 152.11, 146.83, 146.37, 143.19, 139.60, 136.63, 132.61, 132.33, 131.57, 131.11, 129.01, 127.93, 117.60, 117.38, 113.47, 107.74, 29.01. MS (ESI) *m/z* calcd for [M-4Na]<sup>4-</sup> C<sub>46</sub>H<sub>26</sub>N<sub>5</sub>BrO<sub>13</sub>S<sub>4</sub>Zn<sup>4-</sup>: 281.7227, 282.2222. Found: 281.7230, 282.2278. Anal. Calcd (%) for C<sub>46</sub>H<sub>26</sub>N<sub>5</sub>BrNa<sub>4</sub>O<sub>13</sub>S<sub>4</sub>Zn: C, 45.21; H, 2.14; N, 5.73. Found: C, 45.28; H, 2.08; N, 5.72.

#### 5. Synthesis of probe ZPSN

Compound (2) (0.327 g, 0.29 mmol), KI (0.03 g, 0.18 mmol) and *N,N*-diisopropylethylamine (DIPEA) (0.5 mL) was dissolved in 20 mL DMF under N<sub>2</sub> and heated to reflux. Compound (1) (68.6 mg, 0.35 mmol) was dissolved DMF (10 mL) and was added dropwise to the solution. After refluxing under N<sub>2</sub> atmosphere for 10 h, the mixture was cooled to room temperature and the solvent was removed under reduced pressure to obtain a grayish-green solid. Then the residue was dissolved

in H<sub>2</sub>O and washed with CH<sub>2</sub>Cl<sub>2</sub> for three times. The aqueous layer was combined and concentrated then purified by reversephase column chromatography (RP-18), using a H<sub>2</sub>O/MeOH gradient (0 % MeOH to 80 % MeOH). The final ZPSN as sodium salt was afforded with a 51% yield after lyophilization. <sup>1</sup>H NMR (500 MHz, DMSO-*d*<sub>6</sub>) δ 9.48 (s, 1H), 8.80-8.85 (m, 6H), 8.61-8.64 (m, 1H), 8.24-8.27 (m, 4H), 7.88-8.01 (m, 8H), 7.71-7.77 (m, 4H), 7.09 (d, 1H), 6.87 (d, 1H, *J* = 6.8 Hz), 6.73 (d, 1H, *J* = 6.9 Hz), 6.54 (d, 1H, *J* = 6.8 Hz), 4.28 (s, 2H), 3.79 (s, 2H), 2.96 (2H, t, *J* = 7.6 Hz), 2.88 (2H, t, *J* = 7.4 Hz), 2.66-2.70 (2H, m), 1.22 (3H, t, *J* = 7.2 Hz). <sup>13</sup>C NMR (125 MHz, DMSO-*d*<sub>6</sub>) δ 167.21, 153.81, 146.12, 140.37, 138.25, 136.15, 132.46, 132.13, 131.79, 129.74, 127.55, 120.45, 120.00, 115.90, 112.55, 109.13, 62.92, 60.32, 55.96, 29.12, 25.11, 15.59. MS (ESI) *m/z* calcd for [M-4Na]<sup>4-</sup> C<sub>56</sub>H<sub>41</sub>N<sub>7</sub>O<sub>13</sub>S<sub>5</sub>Zn<sup>4-</sup>: 310.7670. Found: 310.7679. Anal. Calcd (%) for C<sub>56</sub>H<sub>41</sub>N<sub>7</sub>Na<sub>4</sub>O<sub>13</sub>S<sub>5</sub>Zn: C, 50.28; H, 3.09; N, 7.33. Found: C, 50.20; H, 3.12; N, 7.41.

## 6. Synthesis of PSN

The metal free control compound PSN was synthesized using the same method as ZPSN by starting from 2-Amino-5,10,15,20-tetra-(4-sulfonatophenyl)-porphyrin (β-ATPPS) instead of Znβ-ATPPS. Yield 60.2 %. <sup>1</sup>H NMR (500 MHz, DMSO-*d*<sub>6</sub>) δ 9.89 (s, 1H), 8.78-8.90 (m, 6H), 8.65-8.69 (m, 1H), 8.32-8.36 (m, 4H), 8.09-8.19 (m, 8H), 7.81-7.86 (m, 6H), 7.39 (d, 1H, *J* = 6.9 Hz), 7.17 (d, 1H, *J* = 7.6 Hz), 4.55 (s, 2H), 4.06 (s, 2H), 3.13-3.17 (2H, t, *J* = 7.8 Hz), 2.88 (2H, t, *J* = 7.4 Hz), 2.72-2.74 (2H, m, *J* = 7.2 Hz), 1.27 (3H, t, *J* = 7.6 Hz), -2.85 (s, 2H). <sup>13</sup>C NMR (125 MHz, DMSO-*d*<sub>6</sub>) δ 169.28, 158.37, 153.29, 148.02, 147.73, 139.02, 137.17, 133.93, 133.66, 131.30, 130.87, 129.34, 127.20, 120.02, 119.66, 108.23, 61.71, 59.71, 57.36, 29.33, 25.41, 15.15. MS (ESI) *m/z* calcd for [M-4Na]<sup>4-</sup> C<sub>56</sub>H<sub>43</sub>N<sub>7</sub>O<sub>13</sub>S<sub>5</sub><sup>4-</sup>: 295.2886. Found: 295.2882. Anal. Calcd (%) for C<sub>56</sub>H<sub>43</sub>N<sub>7</sub>Na<sub>4</sub>O<sub>13</sub>S<sub>5</sub>: C, 52.79; H, 3.40; N, 7.69. Found: C, 52.83; H, 3.47; N, 7.75.

## 7. Synthesis of ZPN

The control compound ZPN without thioether segment was synthesized in the same way as ZPSN by using commercial 2-aminomethylpyridine instead of compound (1a). Yield 79.1 %. <sup>1</sup>H NMR (500 MHz, DMSO-*d*<sub>6</sub>) δ 9.46 (s, 1H), 8.89-8.94 (m, 6H), 8.69-8.71 (m, 1H), 8.36-8.40 (m, 4H), 8.05-8.16 (m, 8H), 7.68-7.73 (m, 4H), 7.23 (d, 1H), 7.17 (d, 1H, *J* = 6.9 Hz), 6.86 (d, 1H, *J* = 7.2 Hz), 6.57 (d, 1H, *J* = 7.4 Hz), 4.32 (s, 2H), 4.16 (d, 2H), 3.72-3.76 (m, 1H). <sup>13</sup>C NMR (125 MHz, DMSO-*d*<sub>6</sub>) δ 168.19, 151.38, 146.78, 146.48, 140.63, 137.90, 137.60, 134.86, 134.66, 132.54, 130.22, 127.46, 125.25, 124.95, 120.01, 114.39, 109.06, 53.48, 52.17. MS (ESI) *m/z* calcd for [M-4Na]<sup>4-</sup> C<sub>52</sub>H<sub>33</sub>N<sub>7</sub>O<sub>13</sub>S<sub>4</sub>Zn<sup>4-</sup>: 288.7583. Found: 288.7578. Anal. Calcd (%) for C<sub>52</sub>H<sub>33</sub>N<sub>7</sub>Na<sub>4</sub>O<sub>13</sub>S<sub>4</sub>Zn: C, 49.99; H, 2.66; N, 7.85. Found: C, 49.75; H, 2.61; N, 7.80.

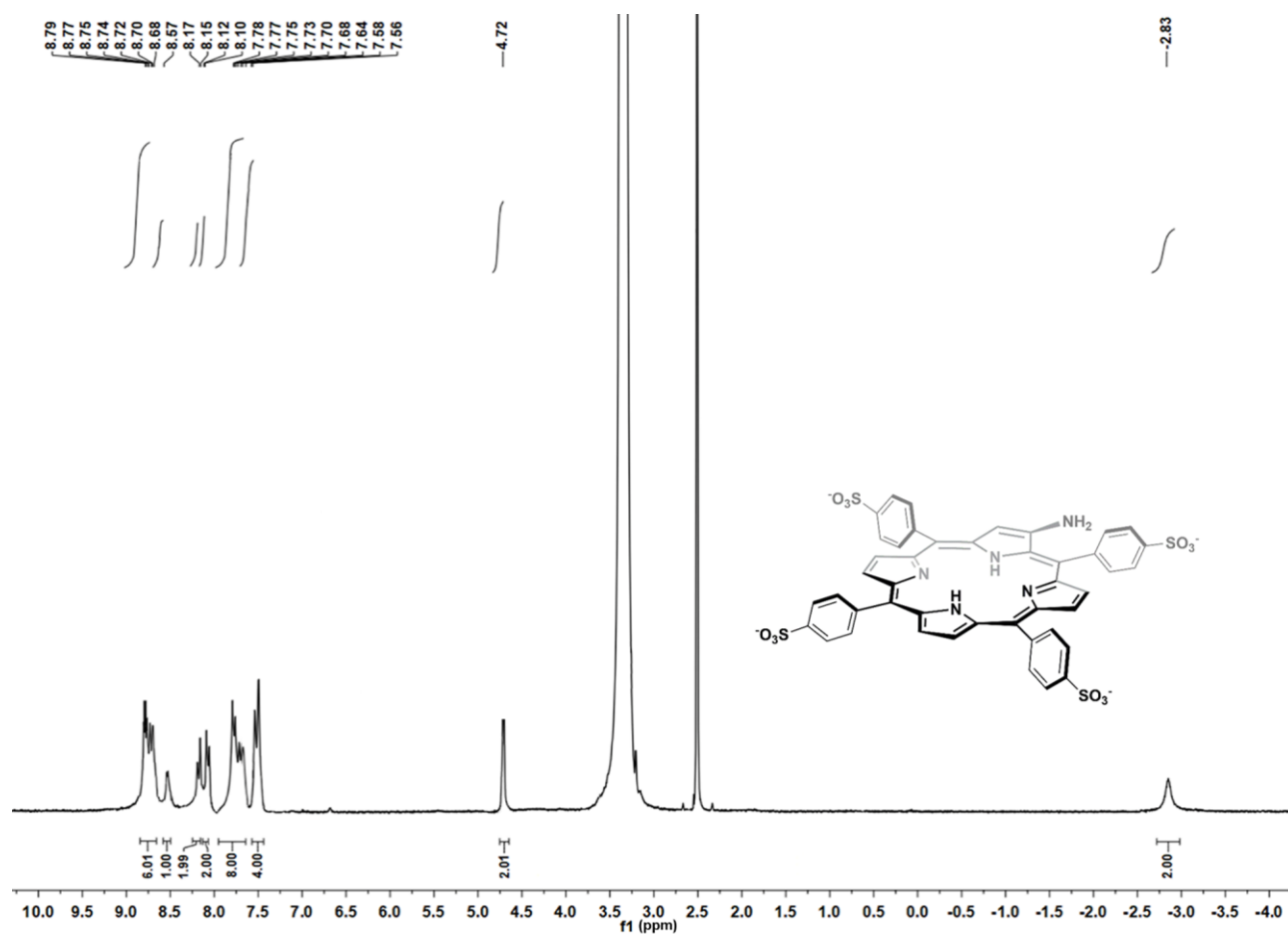


**Figure S1.**  $^1\text{H}$  NMR spectrum of compound  $\beta$ -ATPPS in  $\text{DMSO-}d_6$ .

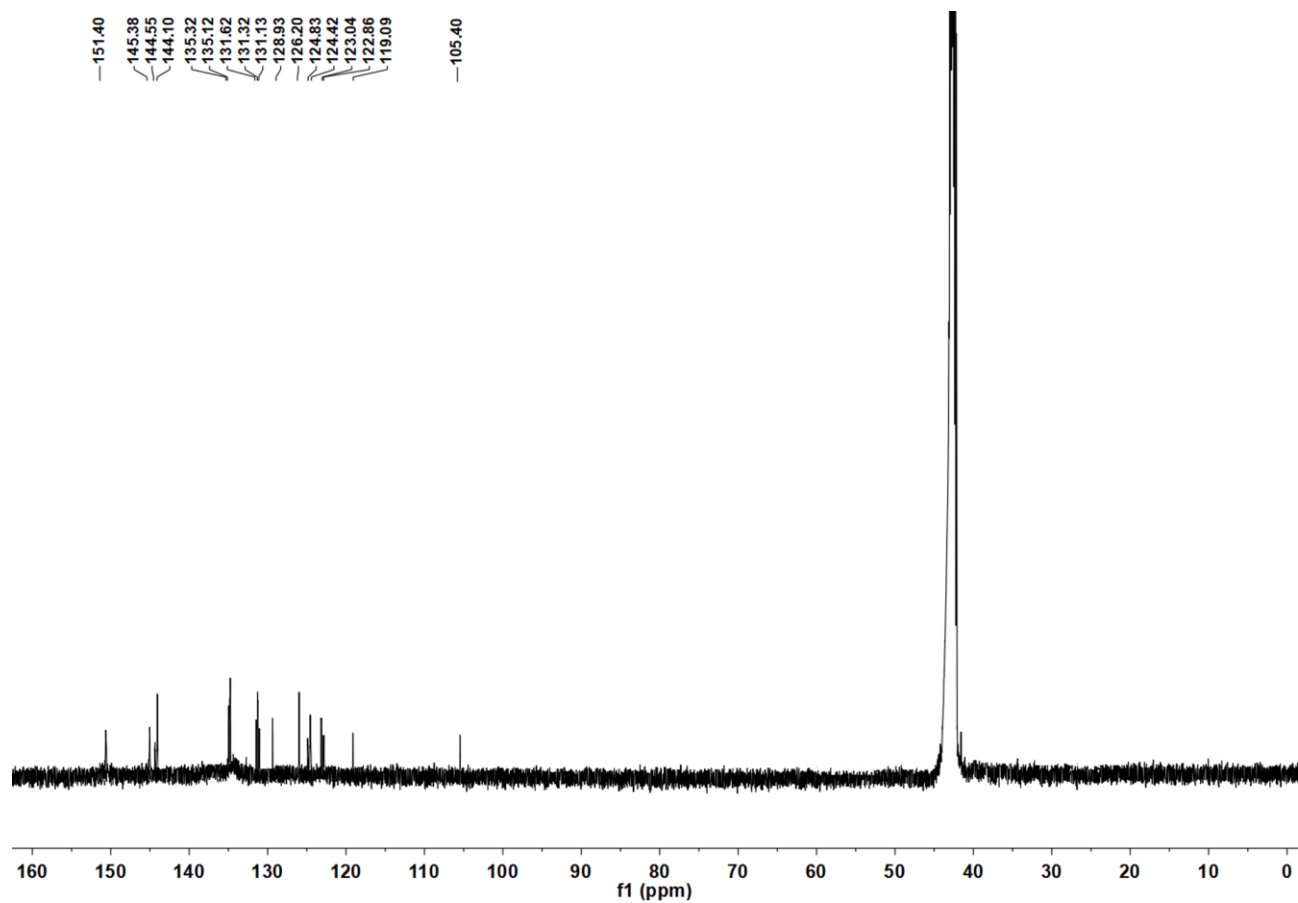


**Figure S2.**  $^{13}\text{C}$  NMR spectrum of compound  $\beta$ -ATPPS in  $\text{DMSO-}d_6$ .

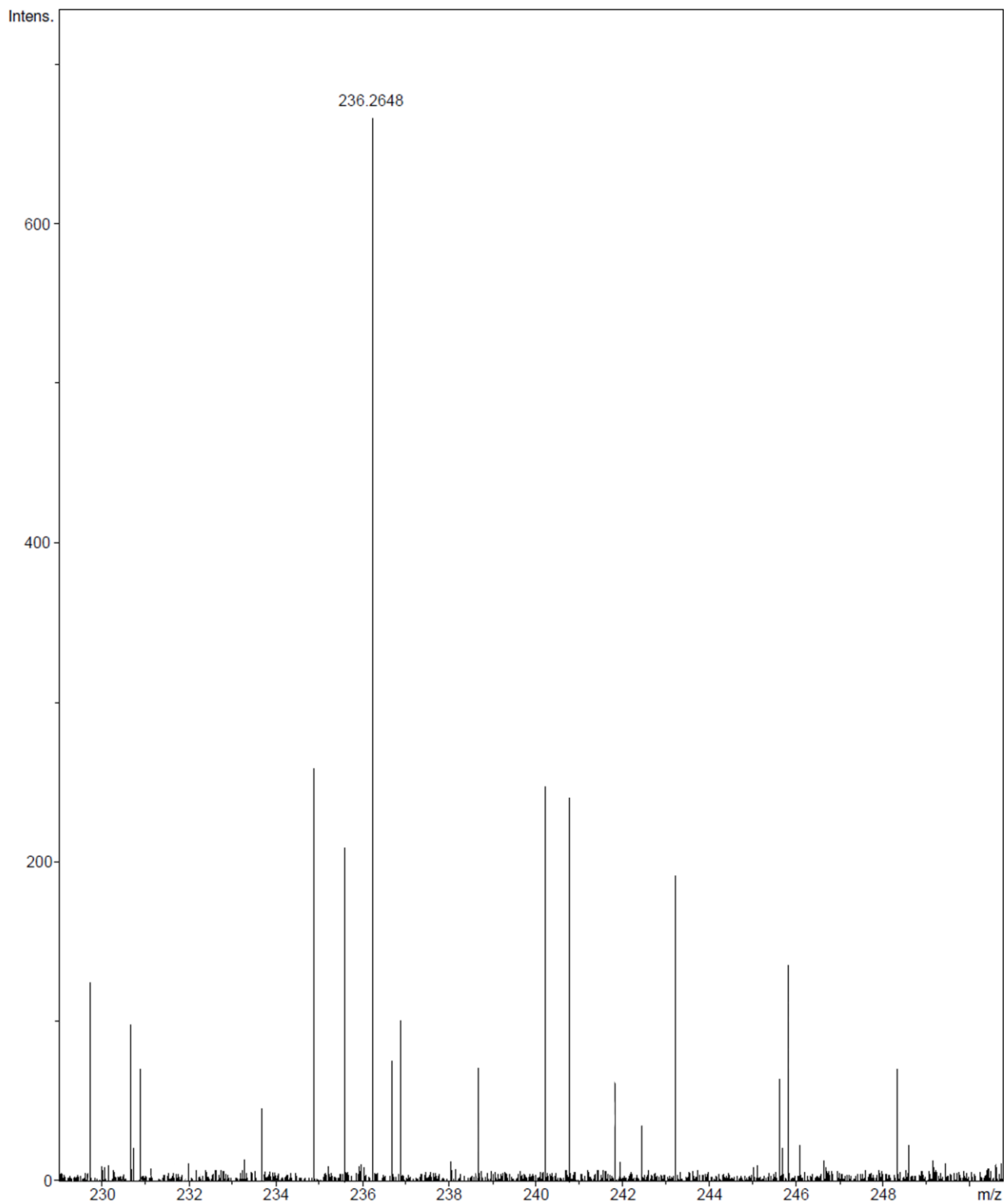


**Figure S3.** Mass spectrum of compound  $\beta$ -ATPPS.

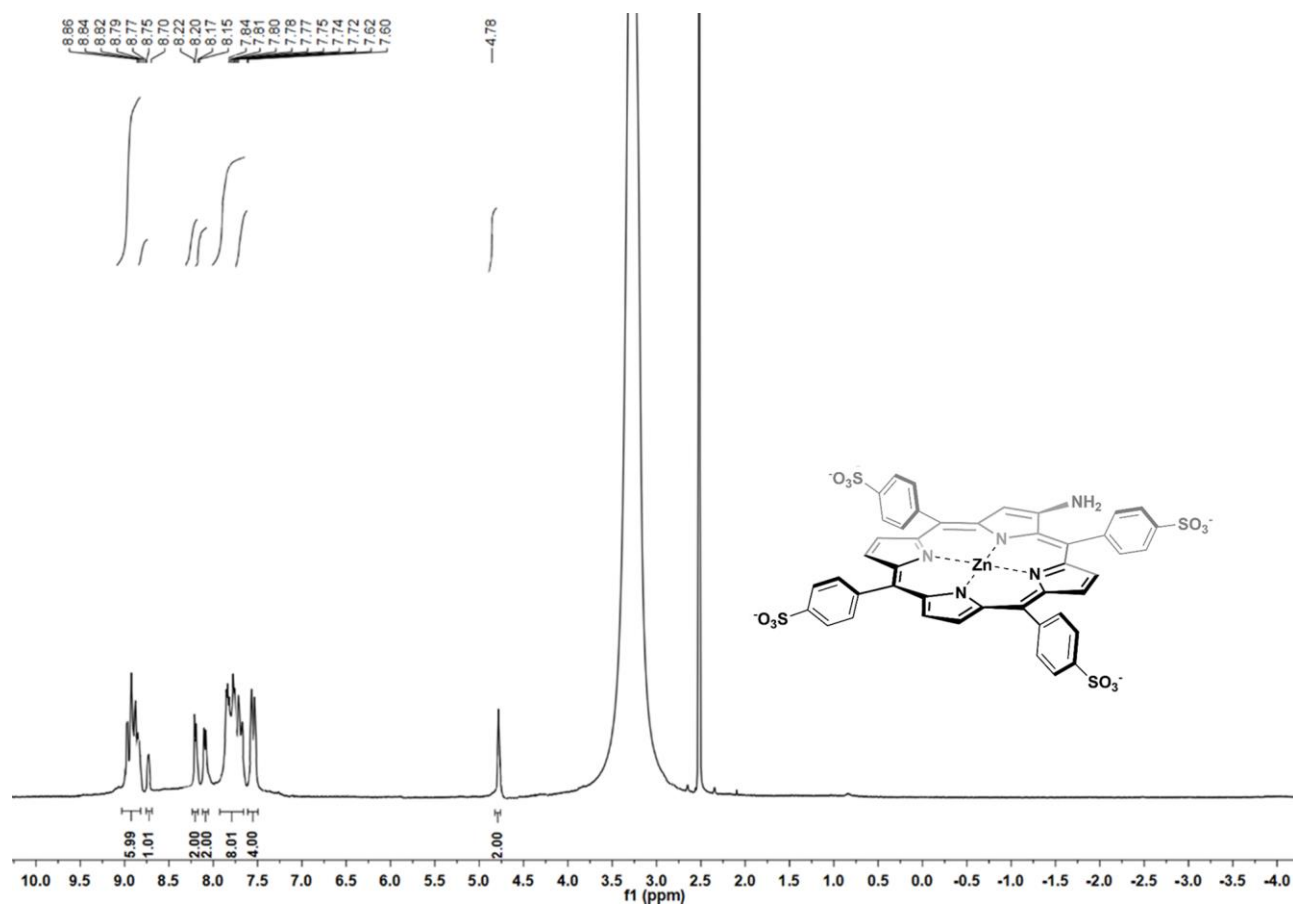


**Figure S4.**  $^1\text{H}$  NMR spectrum of compound  $\text{Zn}\beta\text{-ATPPS}$  in  $\text{DMSO-}d_6$ .

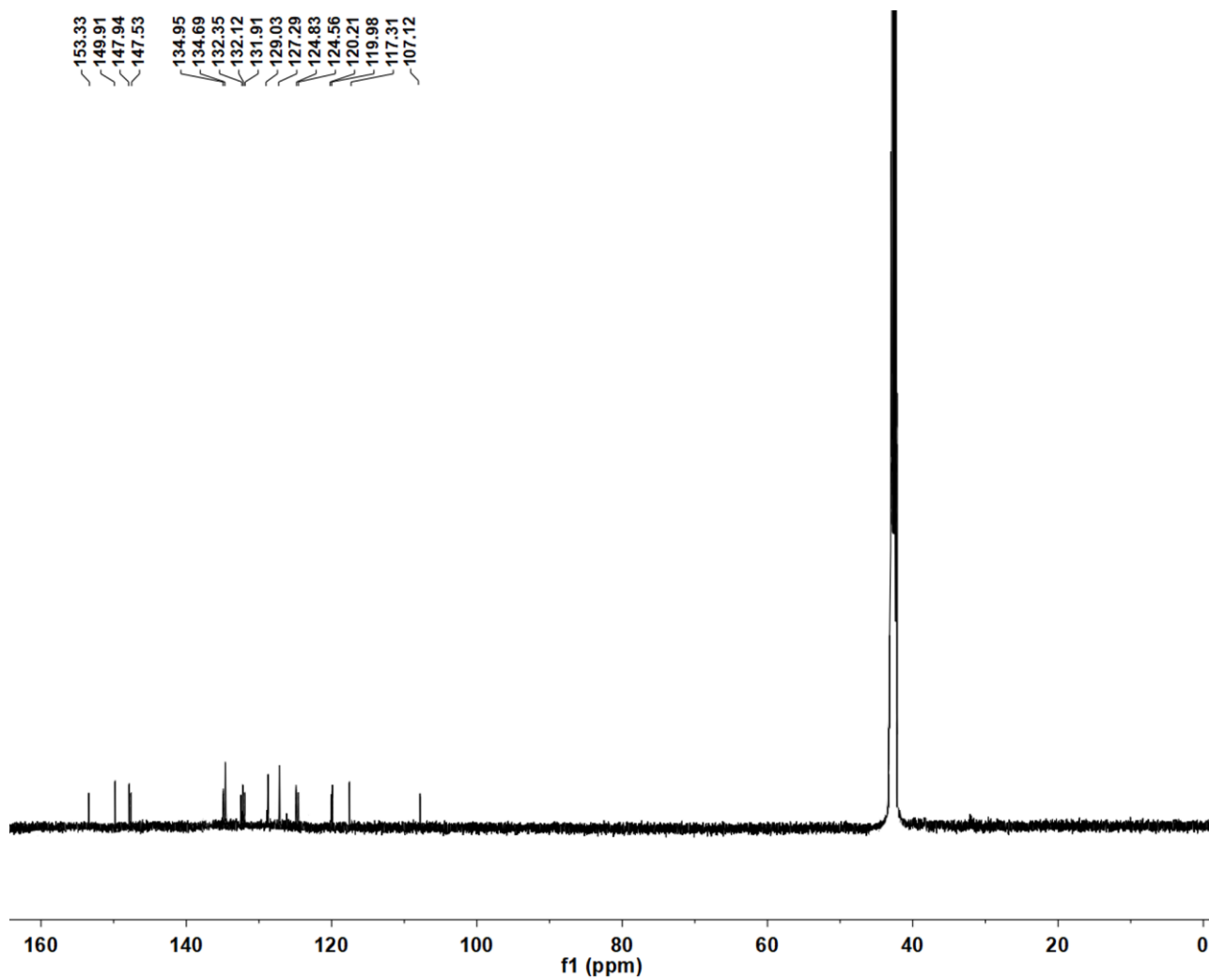


**Figure S5.**  $^{13}\text{C}$  NMR spectrum of compound  $\text{Zn}\beta\text{-ATPPS}$  in  $\text{DMSO-}d_6$ .

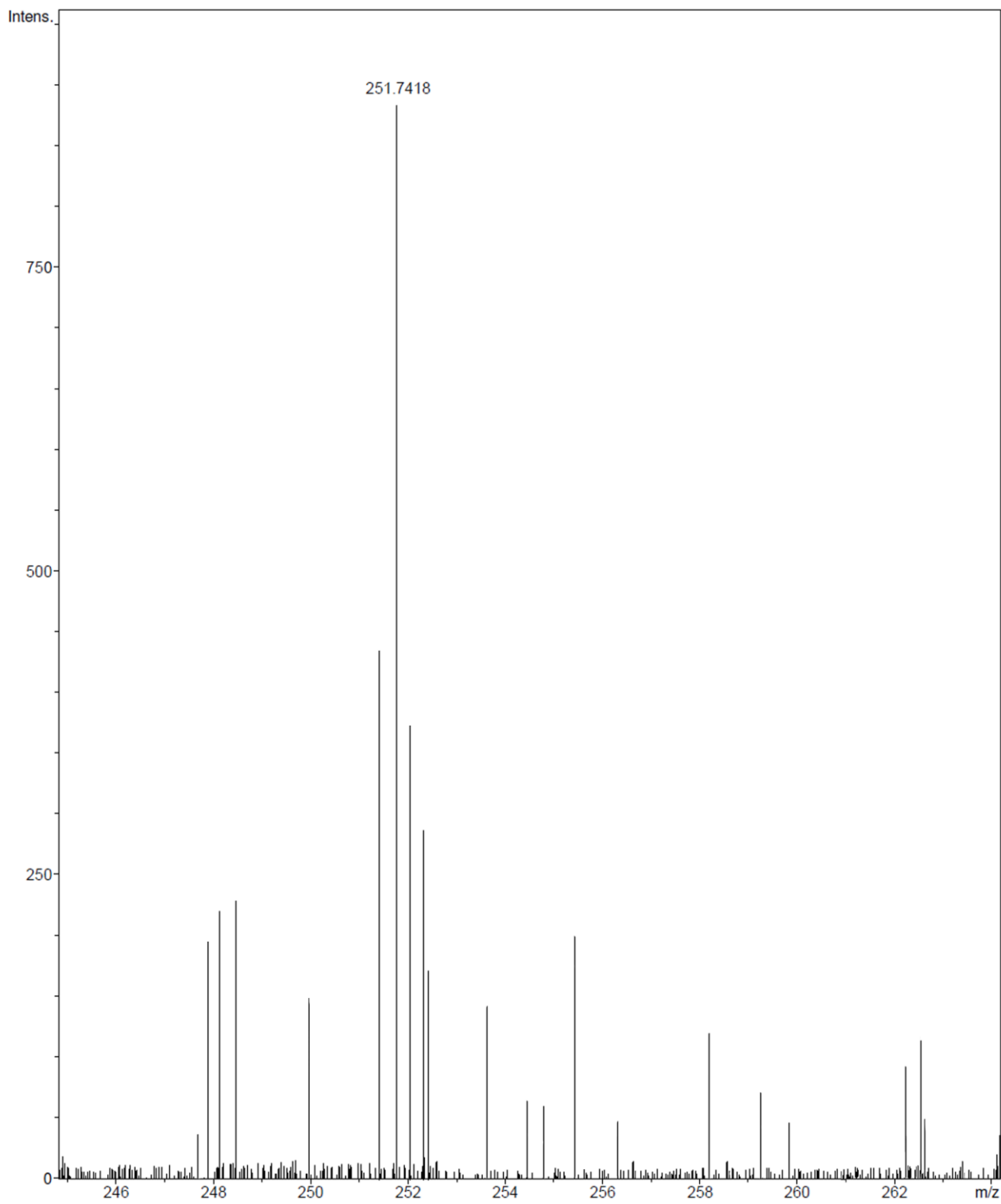


**Figure S6.** Mass spectrum of compound Zn $\beta$ -ATPPS.

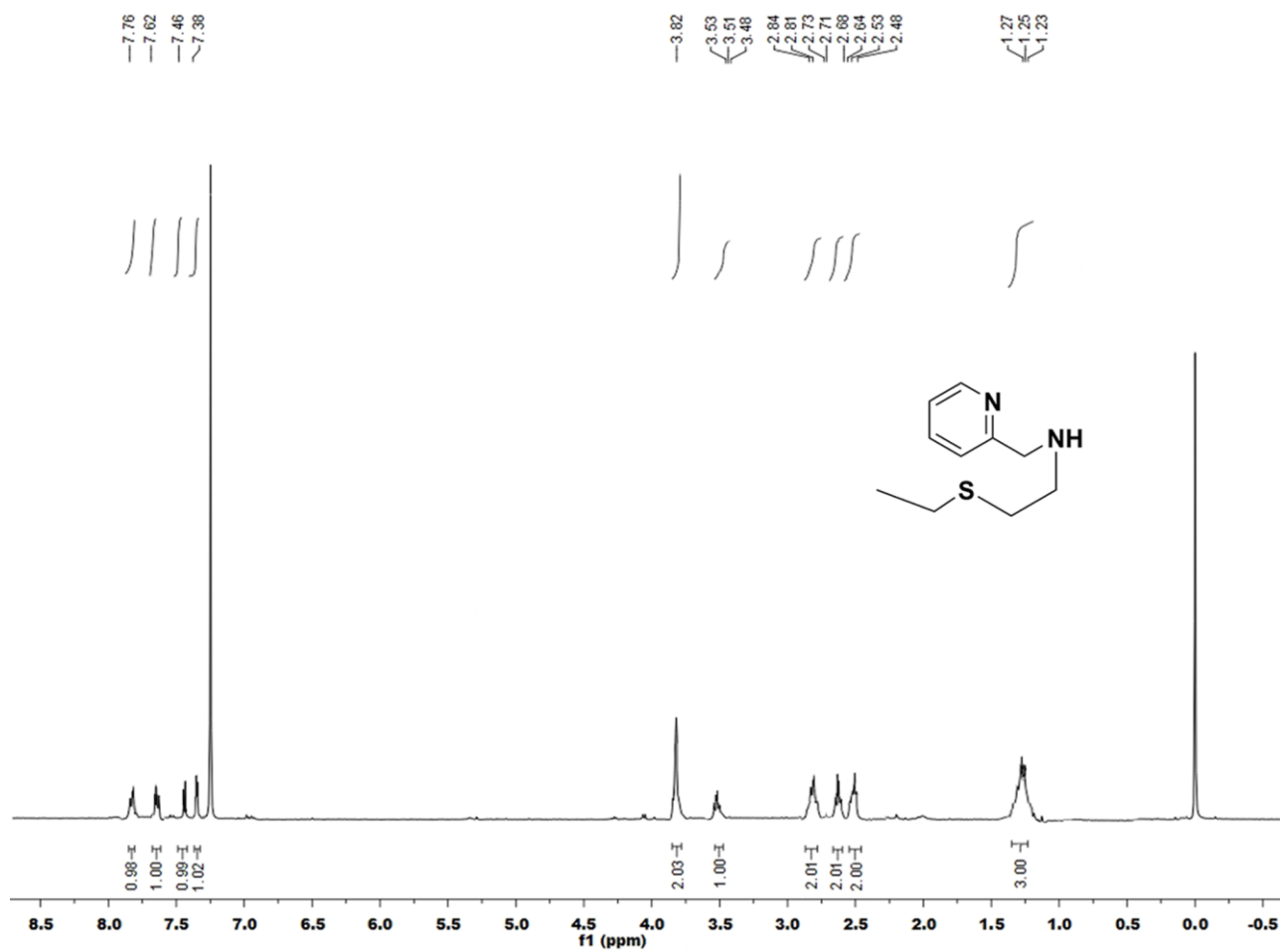


**Figure S7.**  $^1\text{H}$  NMR spectrum of compound (1a) in  $\text{CDCl}_3$ .

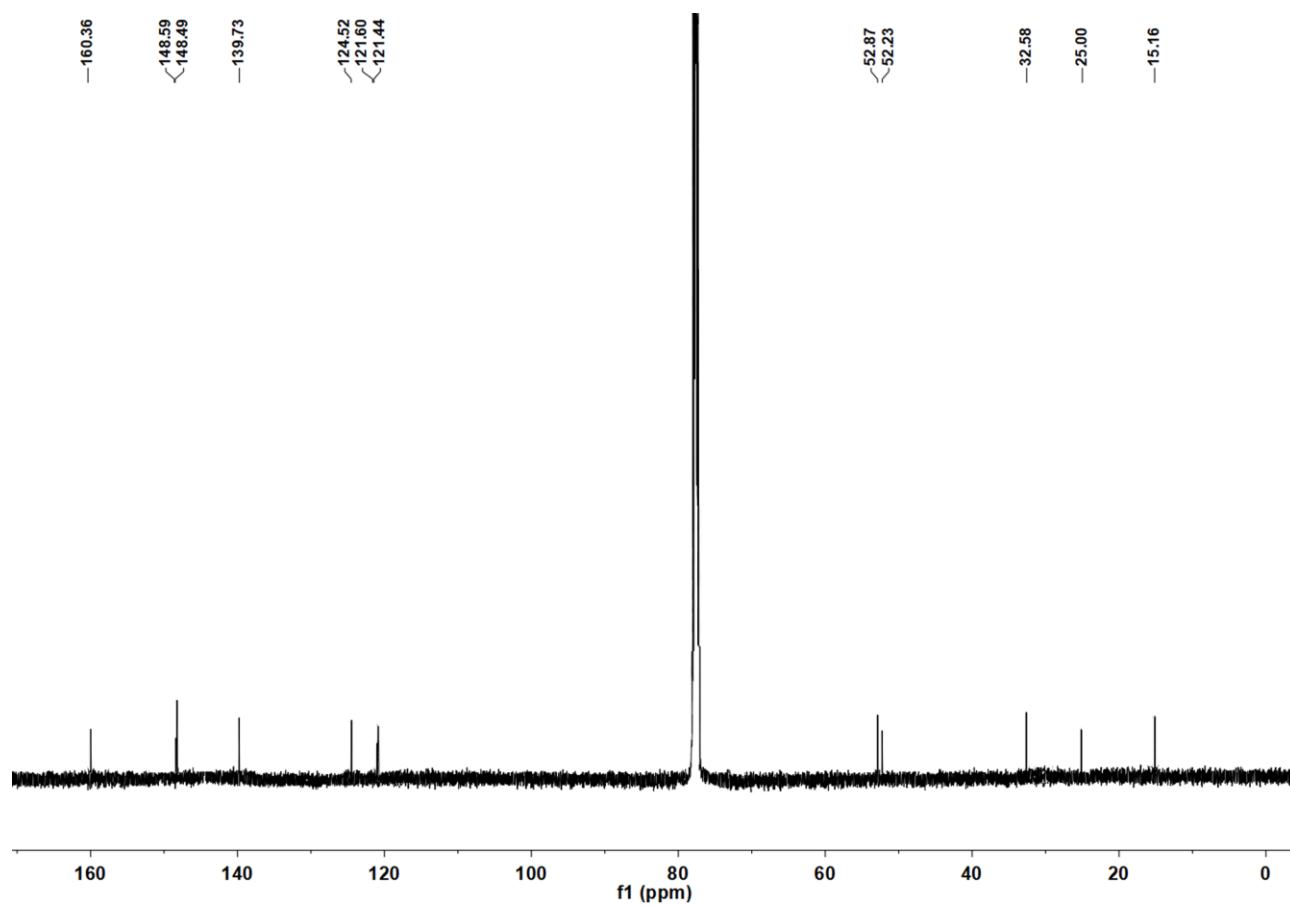


**Figure S8.**  $^{13}\text{C}$  NMR spectrum of compound (1a) in  $\text{CDCl}_3$ .

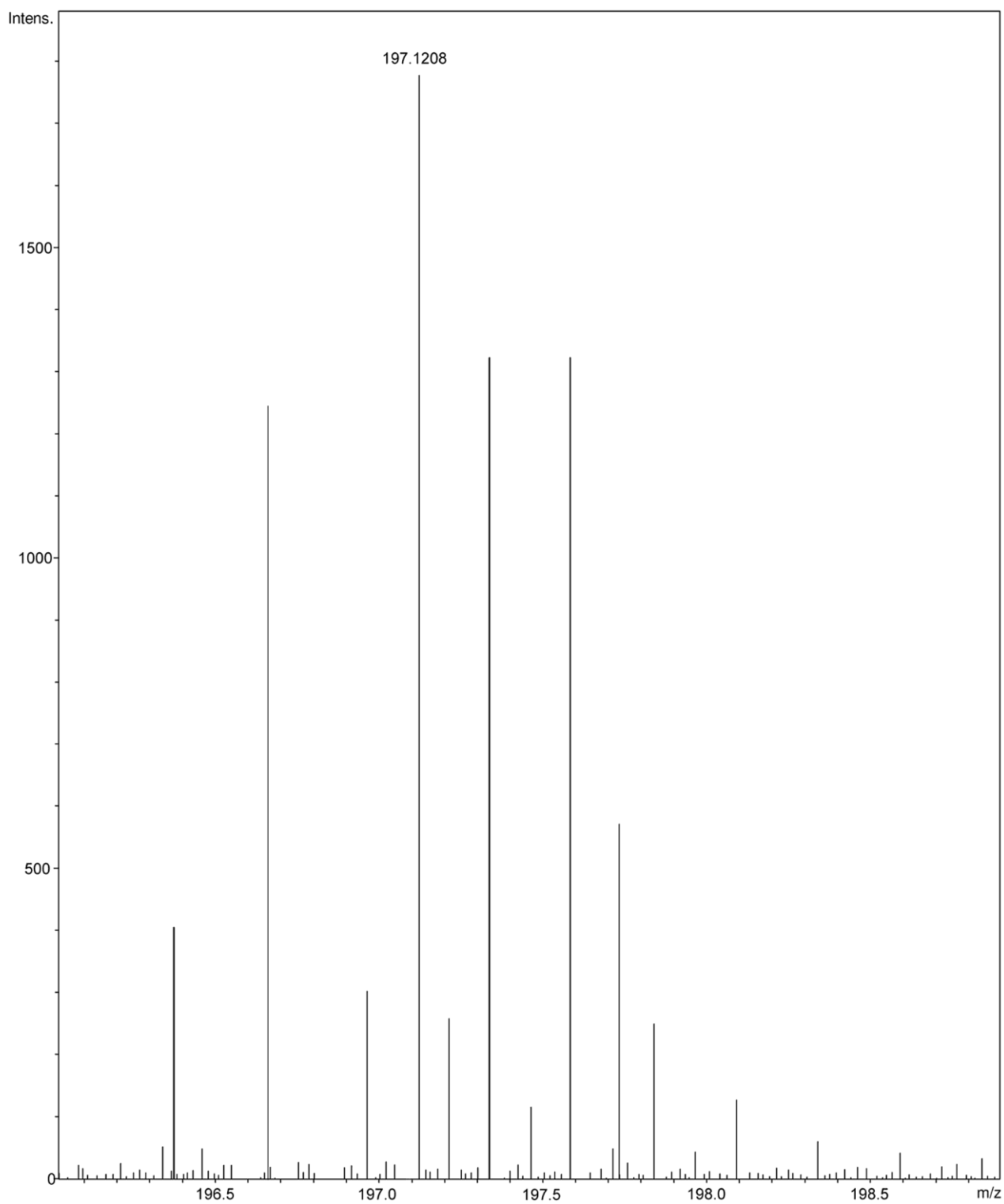


**Figure S9.** Mass spectrum of compound (1a).

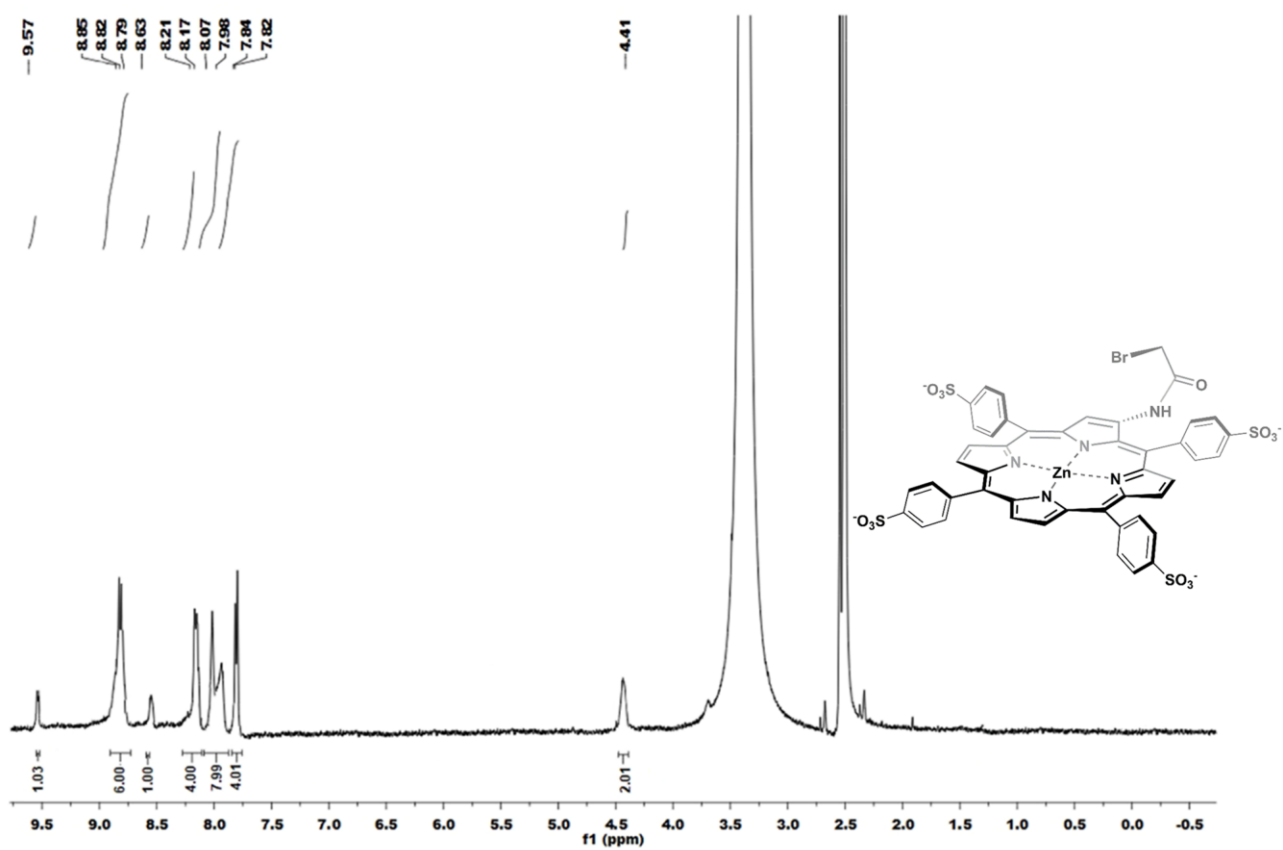


**Figure S10.**  $^1\text{H}$  NMR spectrum of compound (2) in  $\text{DMSO-}d_6$ .

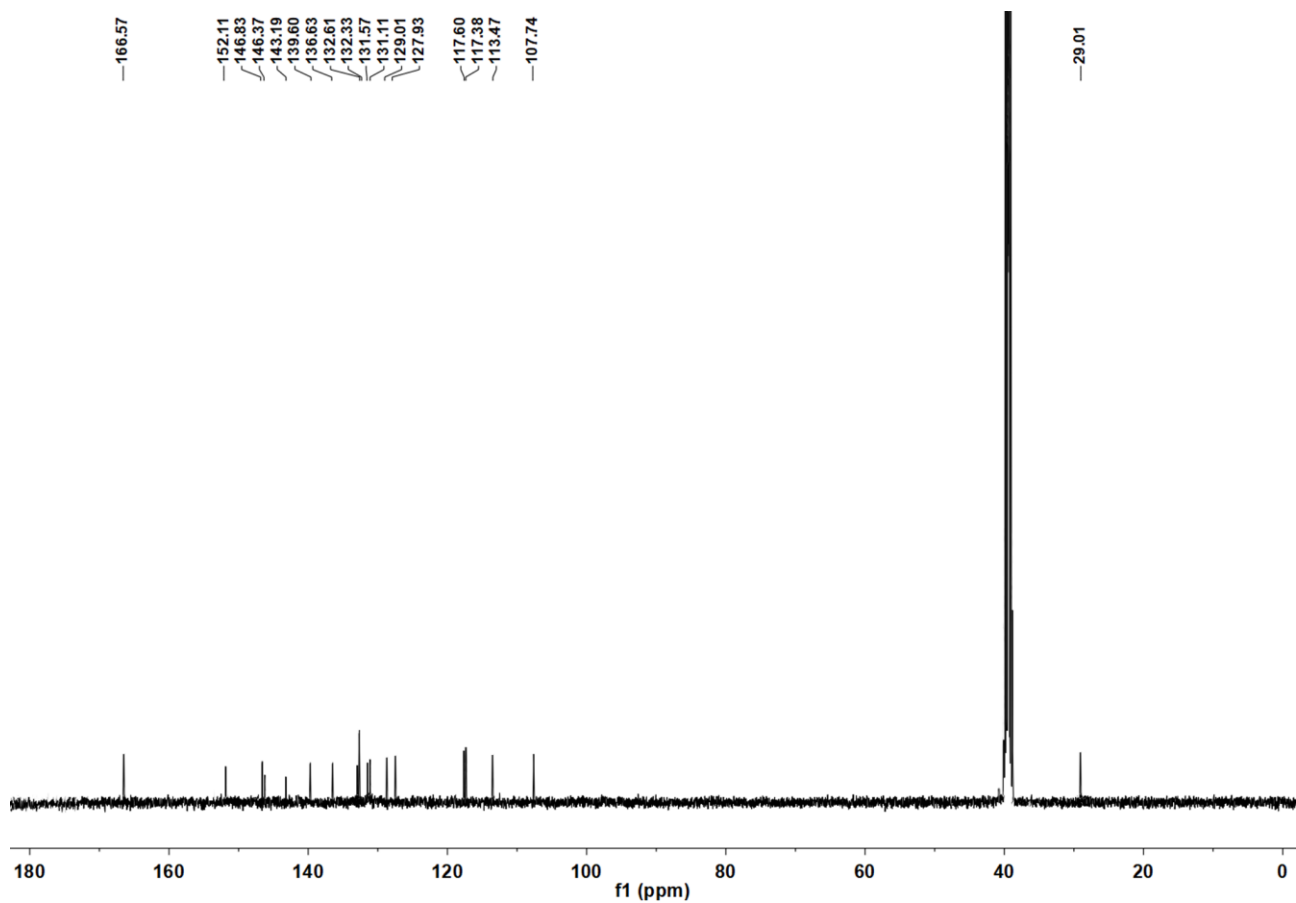


**Figure S11.**  $^{13}\text{C}$  NMR spectrum of compound (2) in  $\text{DMSO-}d_6$ .

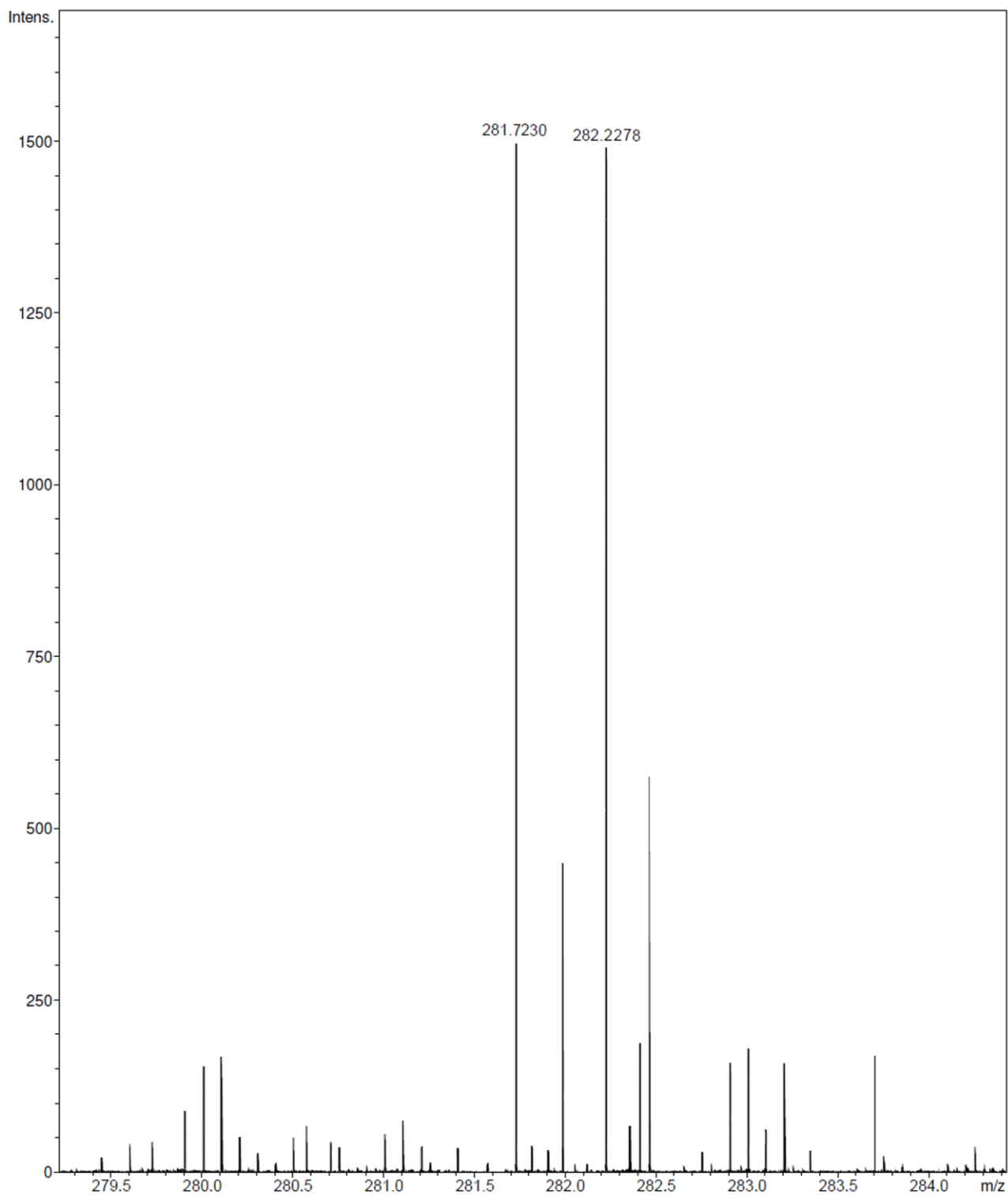


**Figure S12.** Mass spectrum of compound (2).

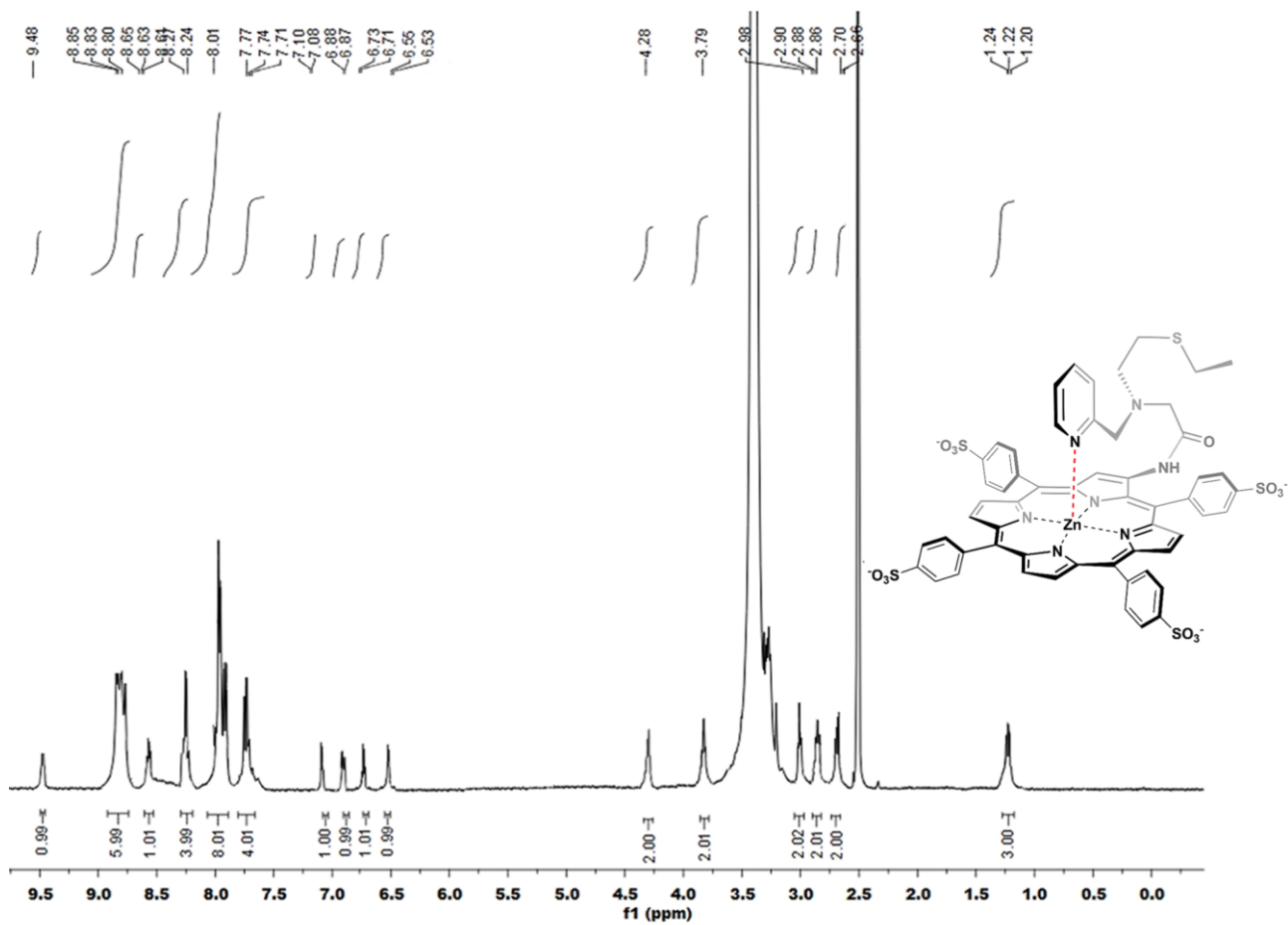


**Figure S13.**  $^1\text{H}$  NMR spectrum of compound ZPSN in  $\text{DMSO-}d_6$ .

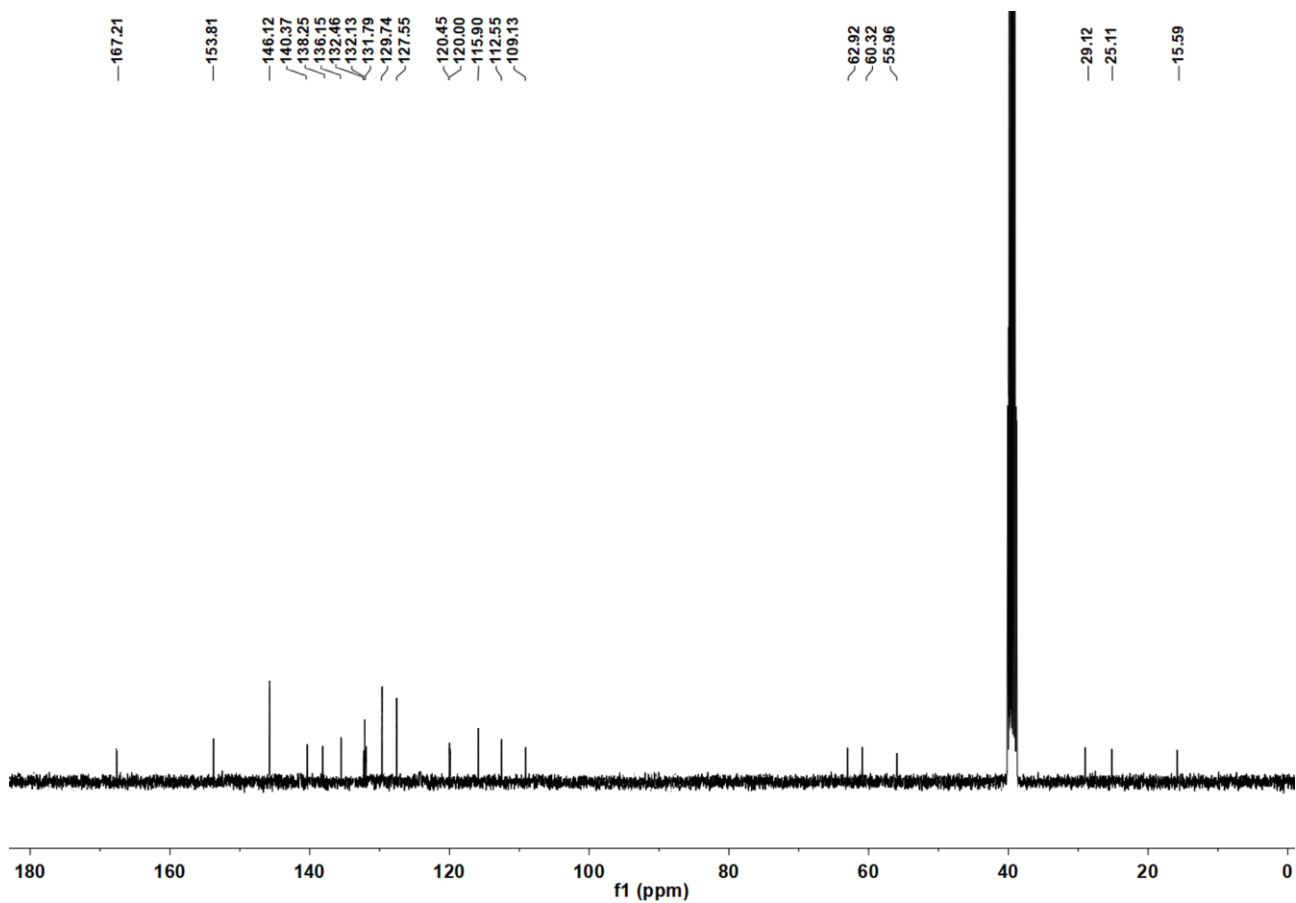


**Figure S14.**  $^{13}\text{C}$  NMR spectrum of compound ZPSN in  $\text{DMSO-}d_6$ .

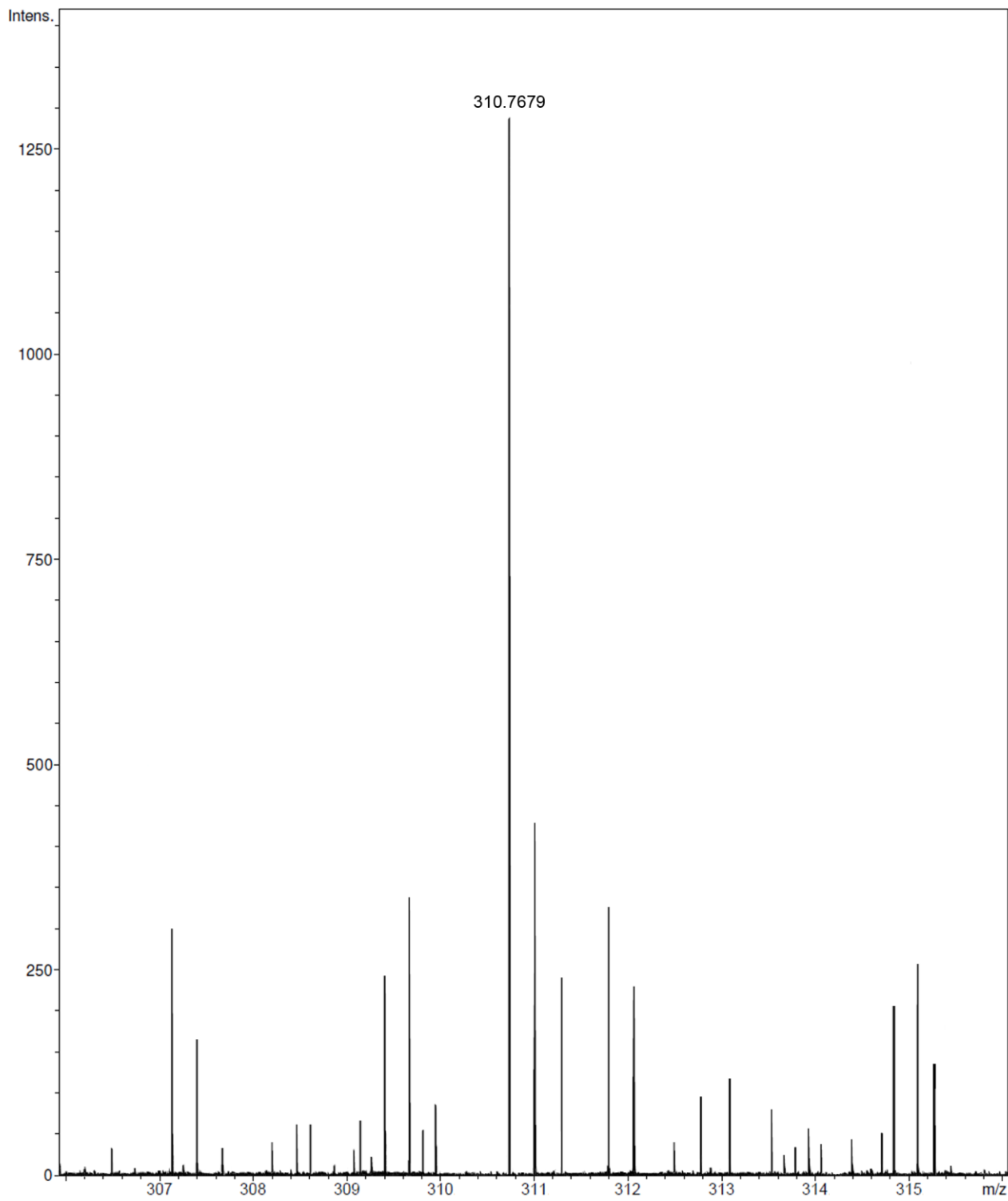


**Figure S15.** Mass spectrum of compound ZPSN.

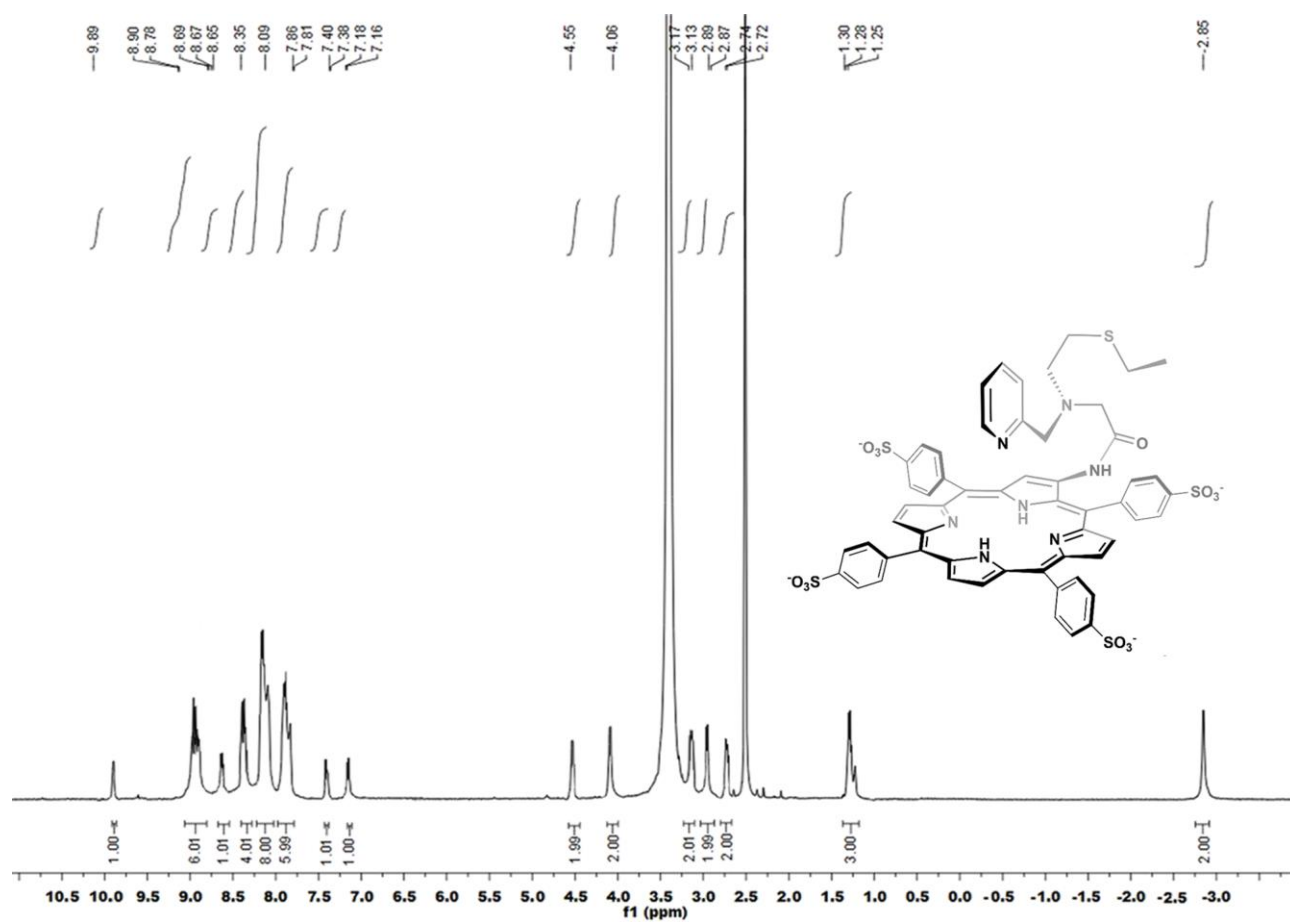


**Figure S16.**  $^1\text{H}$  NMR spectrum of compound PSN in  $\text{DMSO-}d_6$ .

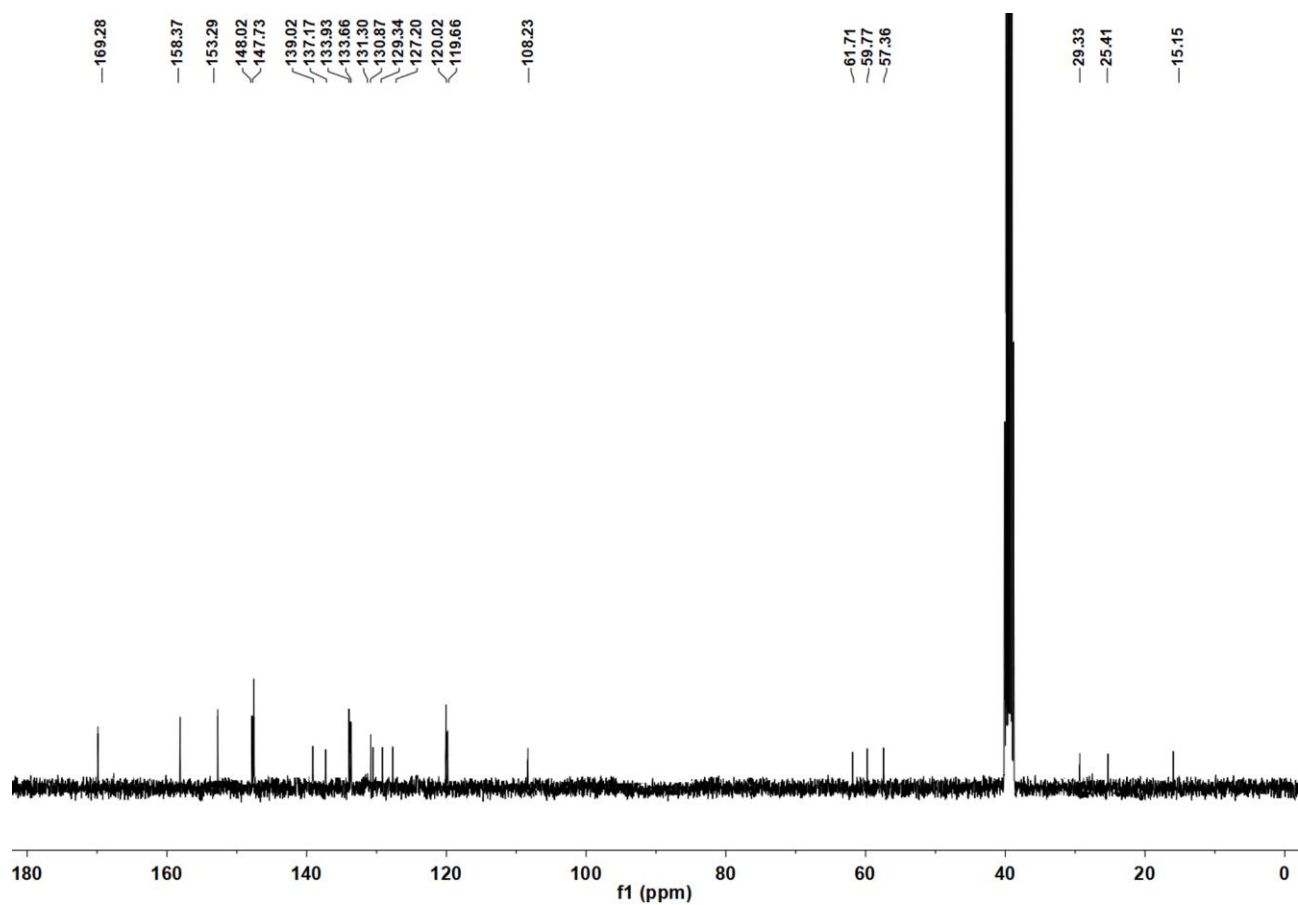


**Figure S17.**  $^{13}\text{C}$  NMR spectrum of compound PSN in  $\text{DMSO-}d_6$ .

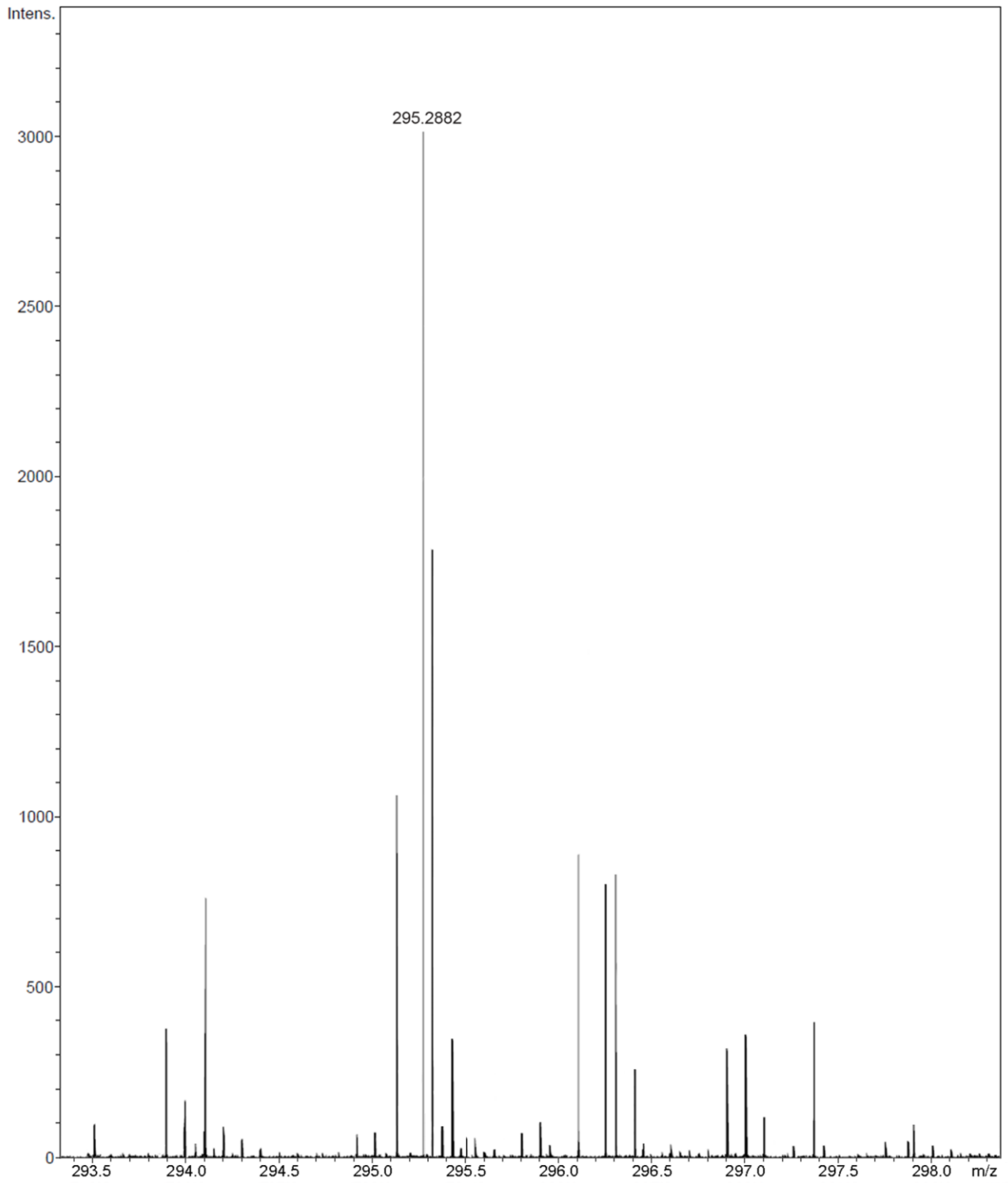


**Figure S18.** Mass spectrum of compound PSN.

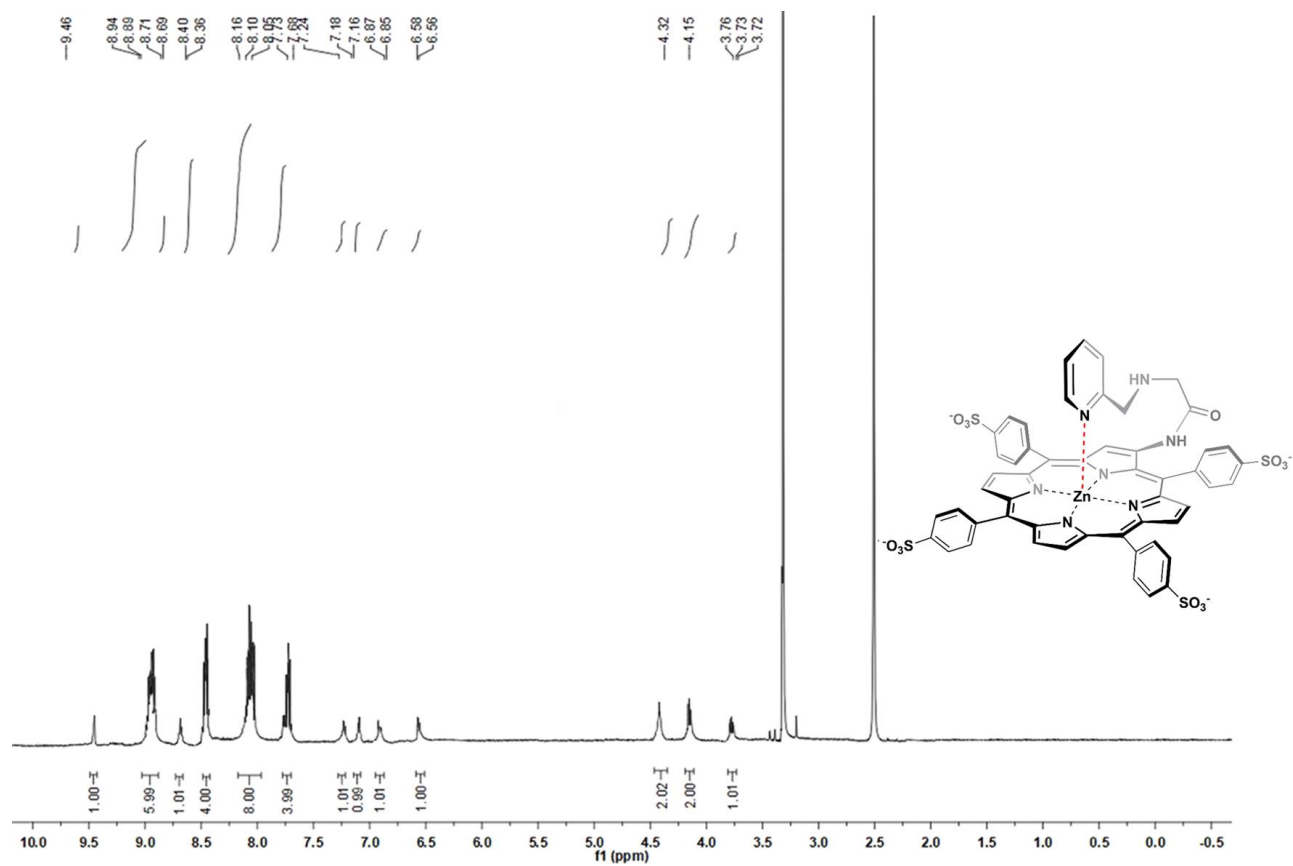


**Figure S19.**  $^1\text{H}$  NMR spectrum of compound ZPN in  $\text{DMSO-}d_6$ .

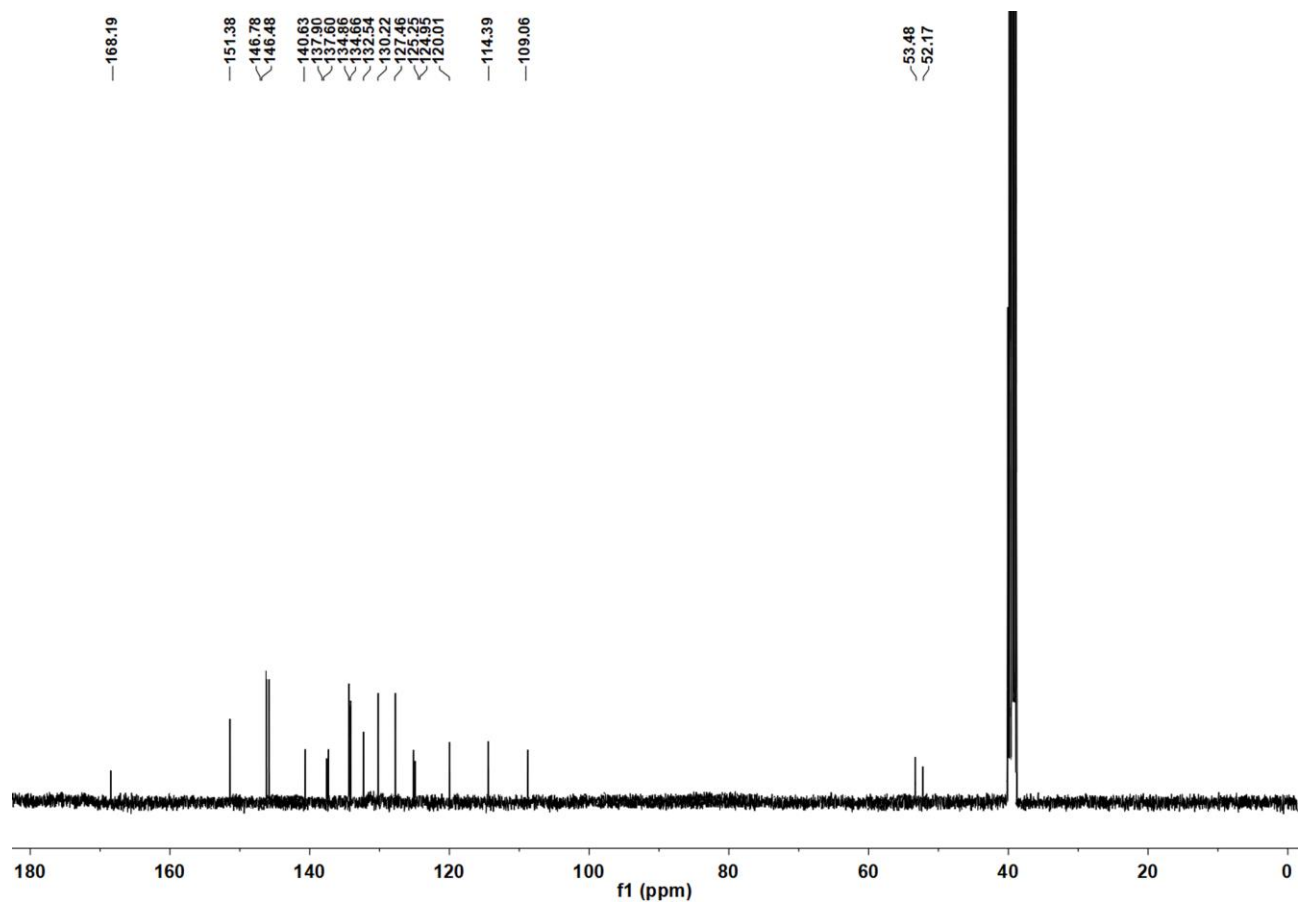


**Figure S20.**  $^{13}\text{C}$  NMR spectrum of compound ZPN in  $\text{DMSO-}d_6$ .

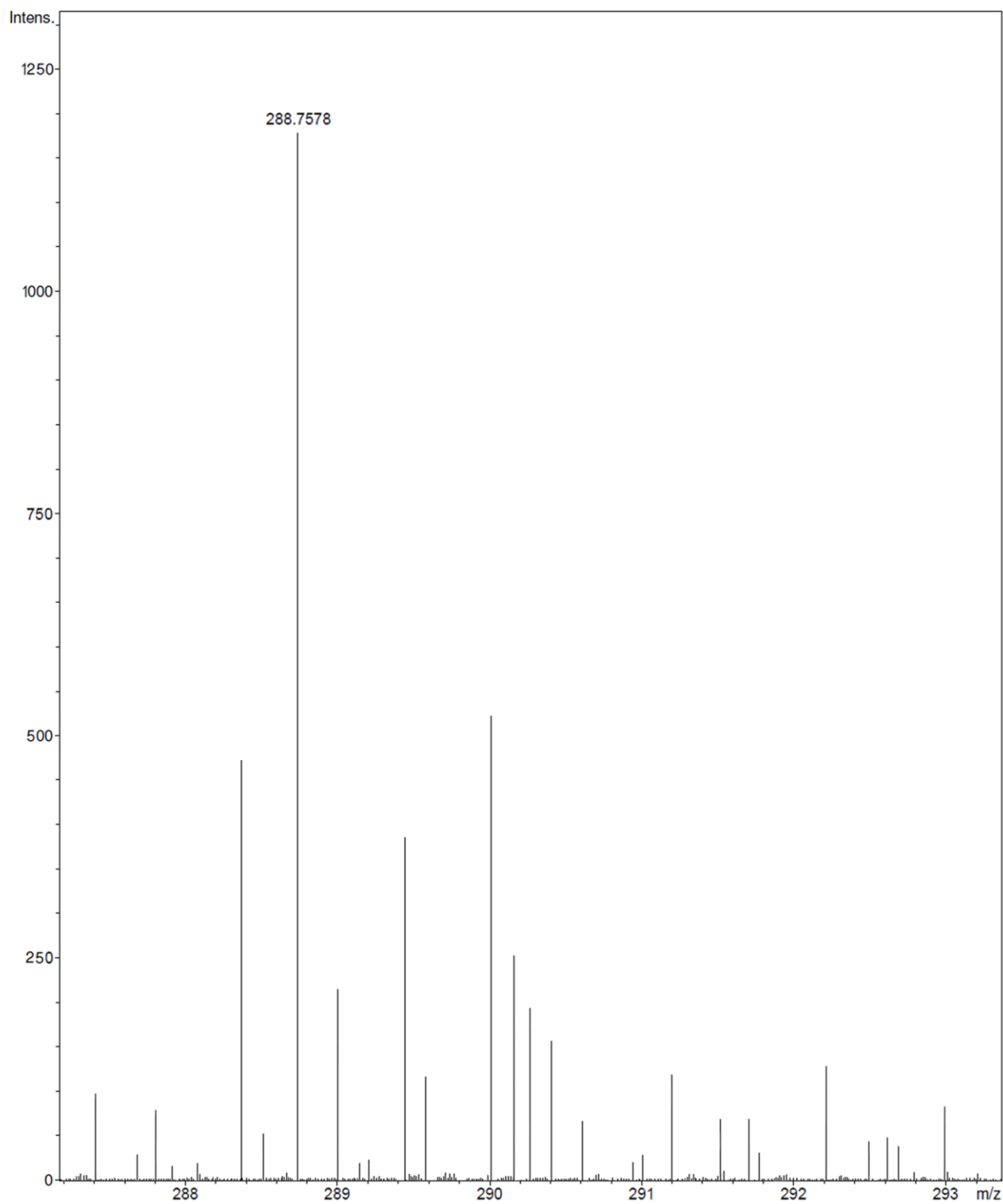


**Figure S21.** Mass spectrum of compound ZPN.

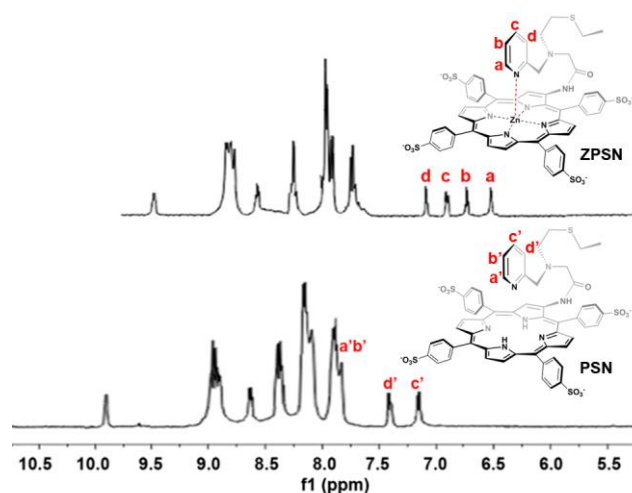


**Figure S22.** Partial  $^1\text{H}$  NMR spectra of compounds ZPSN and PSN in  $\text{DMSO-}d_6$ .

**Solubility of ZPSN in PBS.** To determine whether ZPSN dissolves completely within its testing concentration, different concentrations of ZPSN solutions from 1 to 12  $\mu\text{M}$  in 1  $\mu\text{M}$  interval were prepared by diluting the ZPSN stock solution with PBS (20 mM, pH 7.0). UV-vis absorption spectrum was then scanned from 200 to 800 nm over each solution. By plotting the absorbance intensity at 430 nm against the solution concentration, a maximum concentration in the linear region can be found and taken as the dye solubility.<sup>2</sup> A linear regression equation of calibration curve was also obtained.

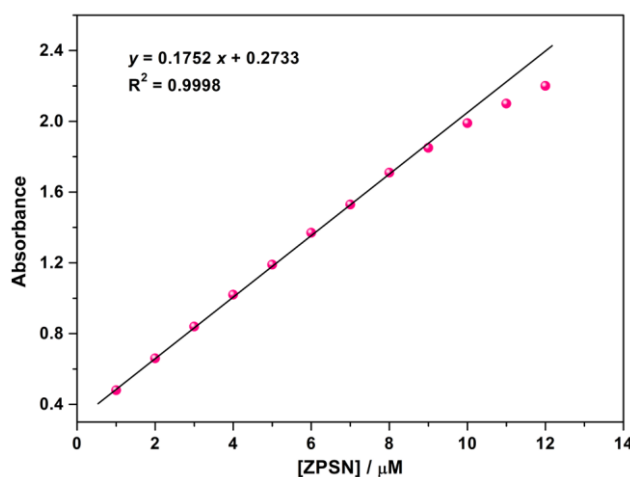


**Figure S23.** Absorbance (at 430 nm) vs. different concentrations of ZPSN in 20 mM PBS at pH 7.0.

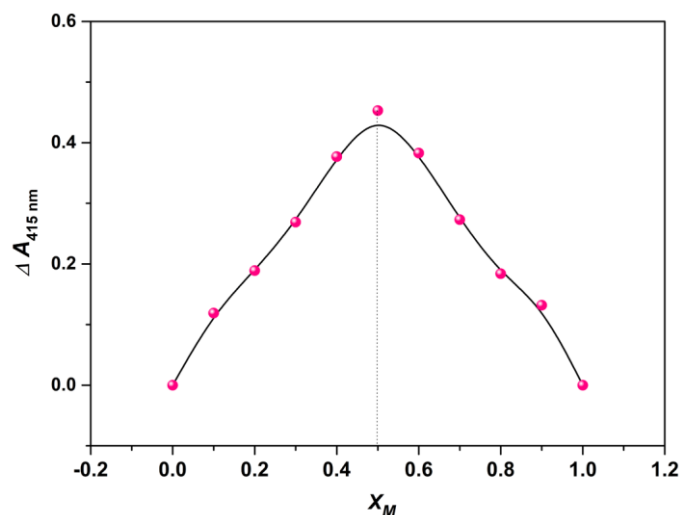


**Figure S24.** Job's plot for ZPSN with  $\text{Cu}^+$  in 20 mM PBS at pH 7.0.  $\Delta A_{415 \text{ nm}}$  is the absorbance changes at 415 nm during titration with a total concentration of ZPSN and  $\text{Cu}^+$  kept at 2  $\mu\text{M}$  ( $X_M = [\text{Cu}^+]/([\text{ZPSN}] + [\text{Cu}^+])$ ).

**Determination of the Dissociation Constant ( $K_d$ ).** The dissociation constant ( $K_d$ ) for binding of  $\text{Cu}^+$  to ZPSN was measured according to the reported method, using thiourea as a competitive ligand. The  $K_d$  value was calculated by using the equation (S2).<sup>3-5</sup>

$$\Delta F = F - F_{\min} = \frac{[\text{Cu}^+](F_{\max} - F_{\min})}{K_d + [\text{Cu}^+]} \quad (\text{S2})$$

where  $F_{\min}$ ,  $F$  and  $F_{\max}$  are the  $\text{Cu}^+$ -elicited fluorescence intensity (at 623 nm) of ZPSN buffered solution (20 mM PBS, pH 7.0, [thiourea] = 0.1 mM) at the initial, intermediate, and the top point, respectively. The concentration of free  $\text{Cu}^+$  in solution was calculated by the stability constants of thiourea from the literature.<sup>6</sup> Plotting  $1/(F - F_{\min})$  against  $1/[\text{Cu}^+]$  could obtain a linear equation as  $y = bx + a$ , and  $K_d$  equals  $b/a$ .

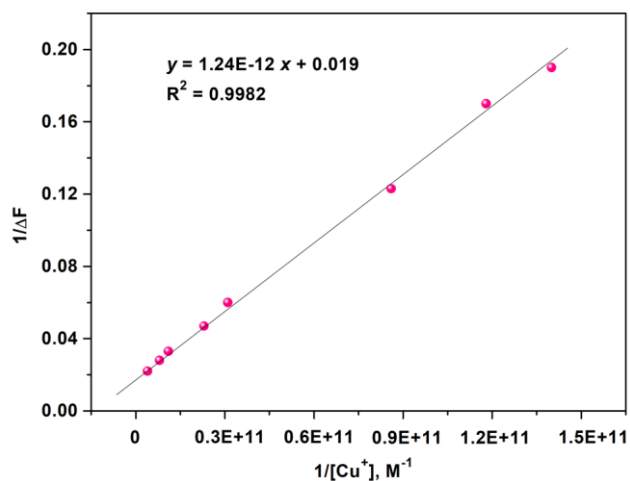


**Figure S25.** Benesi-Hildebrand plot (linear plot) for  $\text{Cu}^+$ -bound ZPSN.

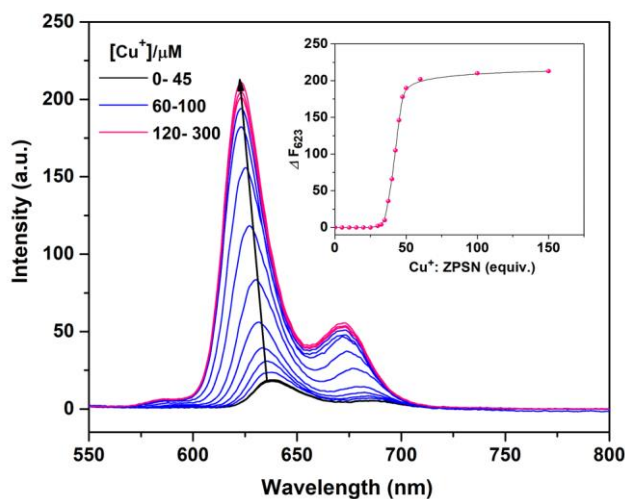


**Figure S26.** Fluorescence response upon titration of  $\text{Cu}^+$  into ZPSN solution ( $2 \mu\text{M}$ ) in PBS ( $20 \text{ mM}$ ,  $\text{pH } 7.0$ ) in the presence of GSH ( $1 \text{ mM}$ ). Inset: plot of  $\Delta F_{623}$  versus ( $\text{Cu}^+$ : ZPSN) for the titration of ZPSN ( $2 \mu\text{M}$ ) in the presence of  $1 \text{ mM}$  GSH.

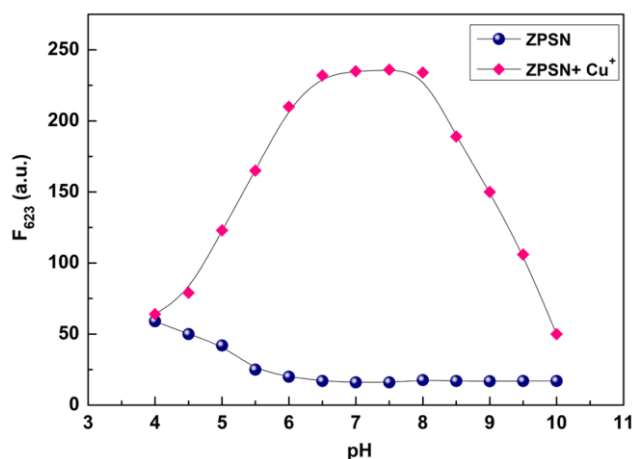


**Figure S27.** Fluorescence emission intensity at 623 nm of free ZPSN (2  $\mu\text{M}$ ) and in the presence of  $\text{Cu}^+$  (1 equiv.) at different pHs.

**Calculation of the Detection Limit.** The detection limit (DL) was calculated based on the fluorescence titration. The standard deviation of blank control was completed when the fluorescence intensity of ZPSN was measured by 10 times. By plotting the concentrations of  $\text{Cu}^+$  against the variation in emission intensities ( $\Delta F$ ), which refers to the difference in the emission intensities of ZPSN at 623 nm before and after exposure to various concentrations of  $\text{Cu}^+$ , yields a linear equation. Three independent duplication measurements of emission intensity were performed in the presence of  $\text{Cu}^+$ . The detection limit was calculated from equation (S3):

$$DL = \frac{3\sigma}{m} \quad (\text{S3})$$

where  $\sigma$  is the standard deviation of the blank experiment, and  $m$  is the slope of the obtained linear equation.

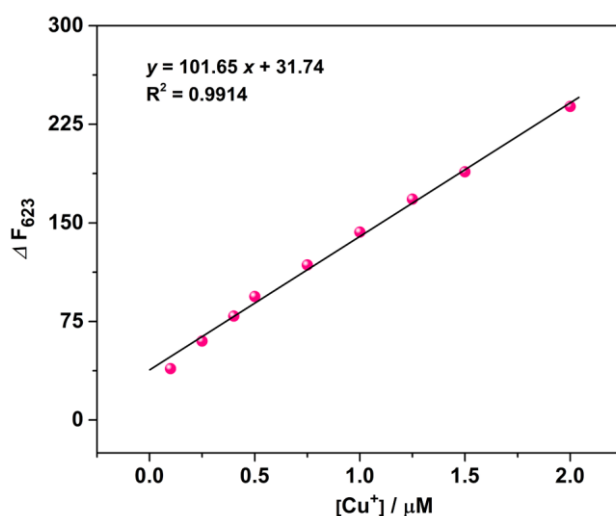


**Figure S28.** Linear calibration curve between the changes in fluorescence intensity at 623 nm ( $\Delta F$ )

and the concentration of  $\text{Cu}^+$ .

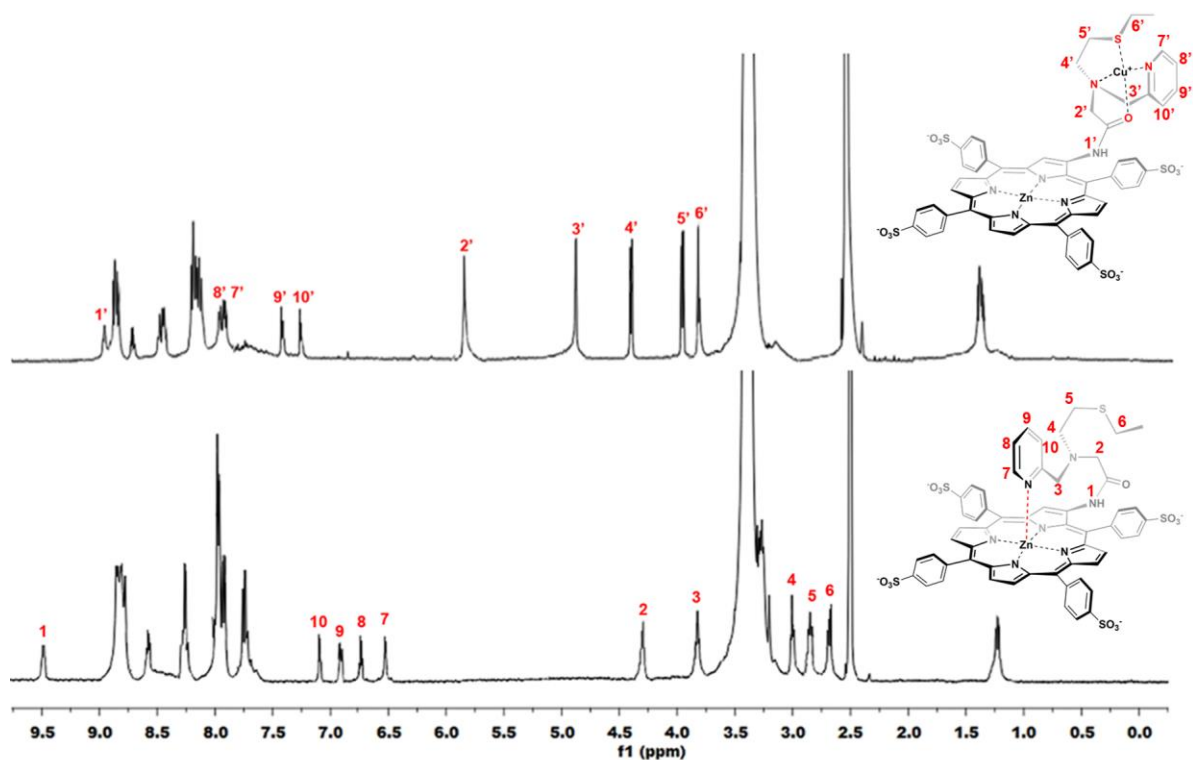


**Figure S29.**  $^1\text{H}$ NMR spectra of ZPSN in the absence and presence of 1 equiv. of  $\text{Cu}^+$  in  $\text{DMSO-}d_6$ .

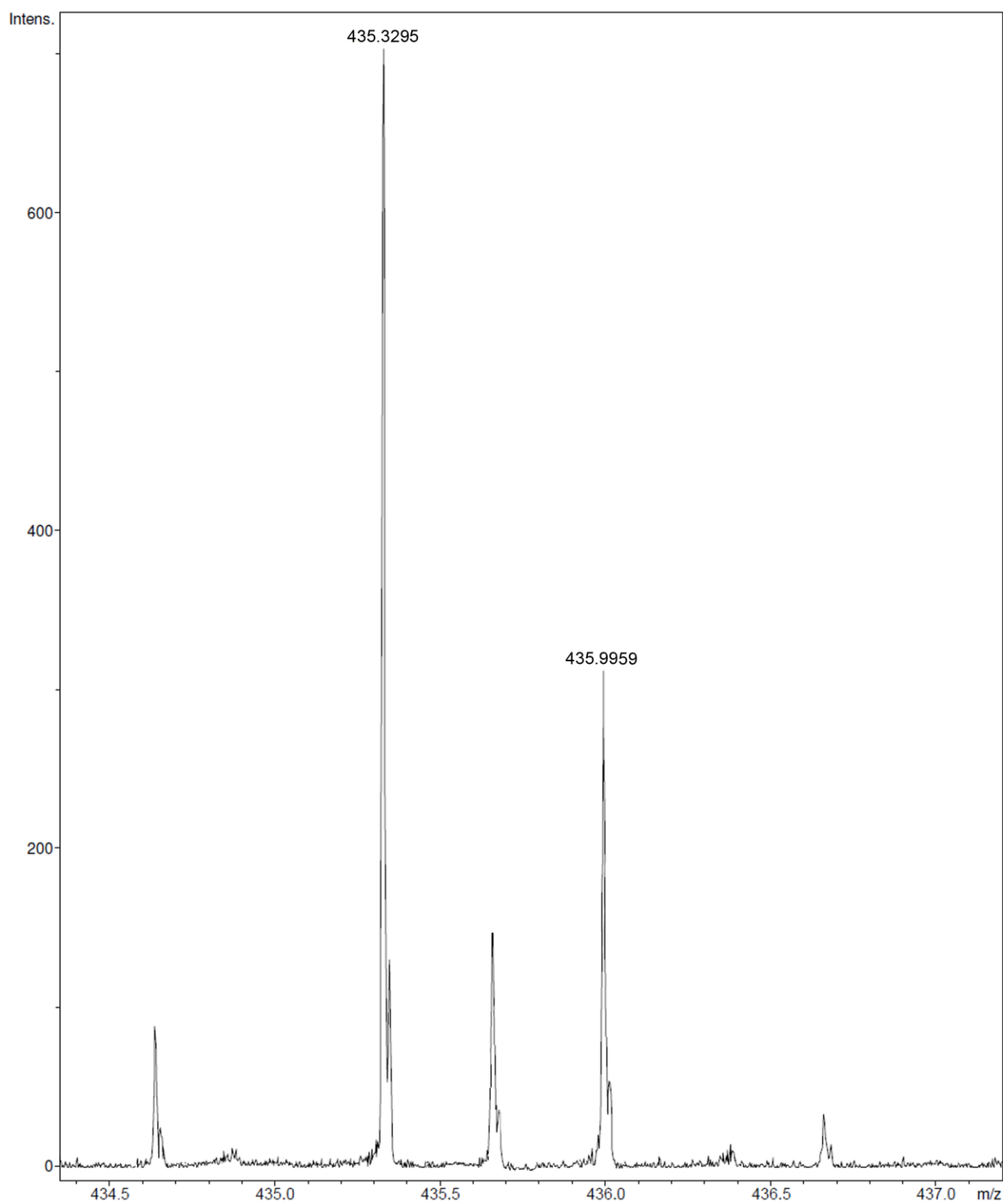


**Figure S30.** Mass spectrum of ZPSN/Cu<sup>+</sup> complex.

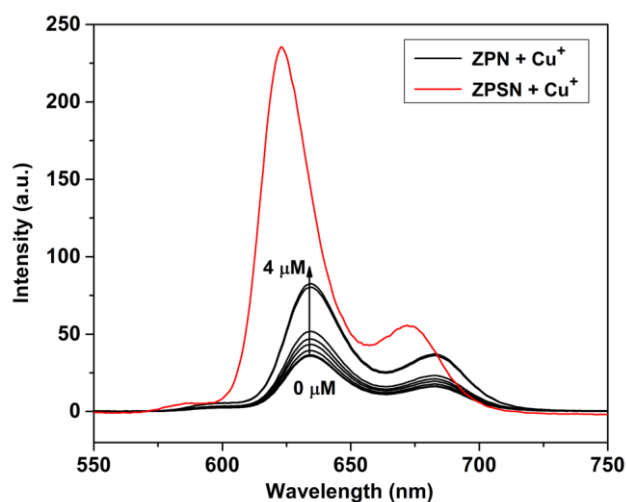


**Figure S31.** Fluorescence spectra of ZPN (2  $\mu\text{M}$ ) and ZPSN (2  $\mu\text{M}$ ) in the presence of  $\text{Cu}^+$  in PBS (20 mM, pH 7.0),  $\lambda_{\text{ex}} = 415 \text{ nm}$ . Black lines: ZPN (2  $\mu\text{M}$ ) with increasing concentrations of  $\text{Cu}^+$  ( $\mu\text{M}$ ) (0, 0.5, 0.75, 1, 1.5, 2, 3, 4); red line: ZPSN (2  $\mu\text{M}$ ) with 4  $\mu\text{M}$   $\text{Cu}^+$ .

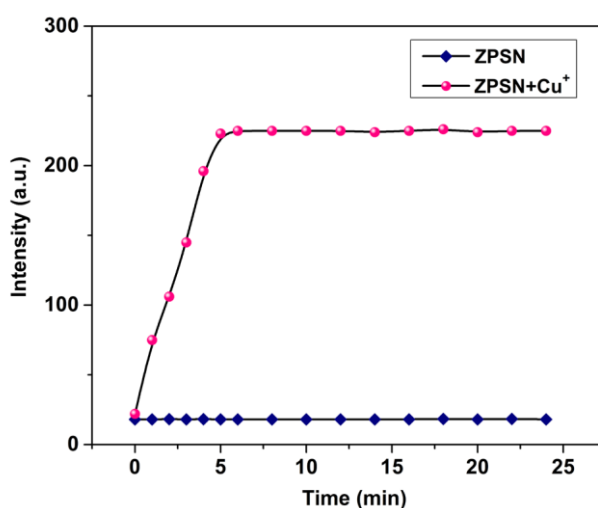


**Figure S32.** Fluorescent intensity of ZPSN (2  $\mu\text{M}$ ) at 623 nm in the absence and upon addition of 1 equiv. of  $\text{Cu}^+$  as a function of time in PBS (20 mM, pH 7.0).

**Cytotoxicity Test.** A standard MTT assay was performed to estimate the cytotoxicity of ZPSN to HeLa cells under our incubation condition. The cultured HeLa cells were firstly rinsed with PBS and treated with increasing concentrations (0, 1, 2, 5, 10, 50, 100  $\mu\text{M}$ ) of ZPSN for 24 hours. Then the supernatants were removed, and the cells were incubated with DMEM medium containing 20 % (V/V) of MTT solution for another 4 hours. Finally, the absorbance intensity was measured at 570 nm using a microplate reader. Untreated cells incubated under the same conditions were used as a control. The relative cell viability (CV %) was the divisor of the absorbance intensity values between samples and the control.

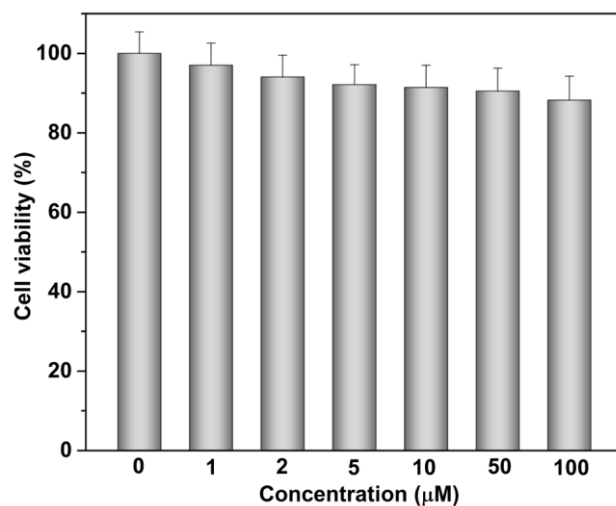


**Figure S33.** Cell viability of HeLa cells with different concentrations of ZPSN (0, 1, 2, 5, 10, 50, 100  $\mu\text{M}$ ) for 24 h.

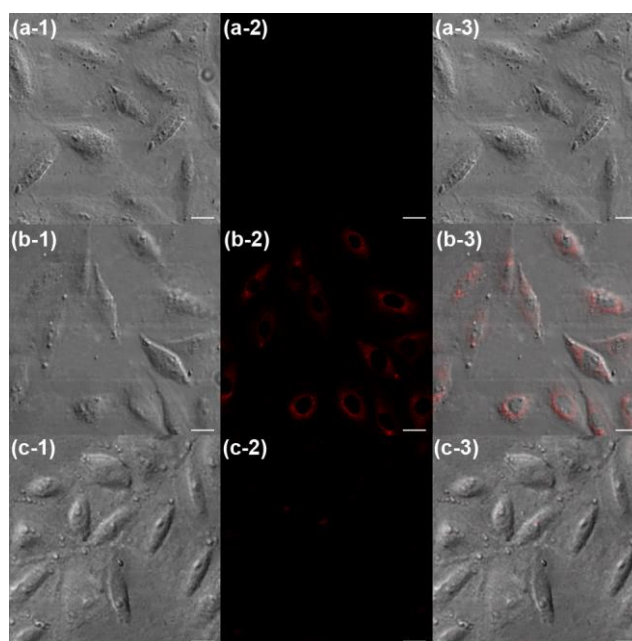


**Figure S34.** Confocal fluorescence imaging of  $\text{Cu}^+$  in A549 cells. (a) Cells incubated with ZPSN (2  $\mu\text{M}$ ) for 20 min; (b) Cells pretreated with 0.1 mM  $\text{CuCl}_2$  in growth media for 7 h at 37  $^\circ\text{C}$  and stained with 2  $\mu\text{M}$  ZPSN for an additional 20 min; (c) Cells pretreated with 0.1 mM  $\text{CuCl}_2$  for 7 h, further incubated with 2  $\mu\text{M}$  ZPSN for 20 min, and subsequently treated with the competing  $\text{Cu}^+$  chelator TAHD (0.1 mM) for 15 min at 37  $^\circ\text{C}$ . (a-1), (b-1), (c-1) Bright-field images; (a-2), (b-2), (c-2) Fluorescence images collected at 600–650 nm; (a-3), (b-3), (c-3) Merged images of the bright field and fluorescence field. (Scale bars, 20  $\mu\text{m}$ ;  $\lambda_{\text{ex}} = 488 \text{ nm}$ ).

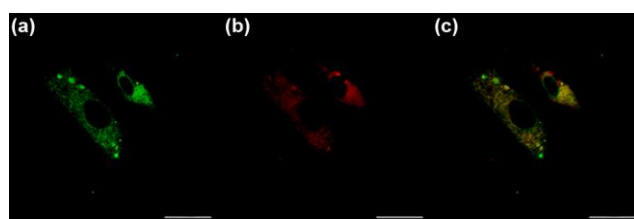


**Figure S35.** Colocalization experiments of ZPSN in mitochondria. Confocal images of A549 cells pretreated with  $\text{CuCl}_2$  (0.1 mM) for 7 h followed by incubation with MitoTracker Green (100 nM) for 20 min and ZPSN (2  $\mu\text{M}$ ) for 20 min. (a) Images were collected at 500–550 nm. (b) Images were collected at 600–650 nm. (c) Colocalized images (Scale bars, 20  $\mu\text{m}$ ;  $\lambda_{\text{ex}} = 488 \text{ nm}$ ).

## References

- (1) Lipińska, M. E.; Teixeira D. M. D.; Laia, C. A. T.; Silva, A. M. G.; Rebelo, S. L. H.; Freire, C.  $\beta$ -Functionalized zinc(II)aminoporphyrins by direct catalytic hydrogenation. *Tetrahedron Lett.* **2013**, *54*, 110–113.
- (2) Morgan, M. T.; Bagchi, P.; Fahrni, C. J. Designed to dissolve: Suppression of colloidal aggregation of Cu(I)-selective fluorescent probes in aqueous buffer and in-gel detection of a metallochaperone. *J. Am. Chem. Soc.* **2011**, *133*, 15906–15909.
- (3) Cao, X. W.; Lin, W. Y.; Wan, W. Development of a near-infrared fluorescent probe for imaging of endogenous  $\text{Cu}^+$  in live cells. *Chem. Commun.* **2012**, *48*, 6247–6249.
- (4) Bao, X. F.; Cao, Q. S.; Wu, X. L.; Shu, H.; Zhou, B. J.; Geng, Y. L.; Zhu, J. Design and synthesis of a new selective fluorescent chemical sensor for  $\text{Cu}^{2+}$  based on a pyrrole moiety and a fluorescein conjugate. *Tetrahedron Lett.* **2016**, *57*, 942–948.
- (5) Benesi, H. A.; Hildebrand, J. H. A spectrophotometric investigation of the interaction of iodine with aromatic hydrocarbons. *J. Am. Chem. Soc.* **1949**, *71*, 2703–2707.
- (6) Smith, R. M.; Martell, A. E. *Critical Stability Constants*, Plenum Press: New York, 1989.